Inorg. Chem. **2006**, *45*, 4136–4149

Mixed Substituted Porphyrins: Structural and Electrochemical Redox Properties

P. Bhyrappa,* M. Sankar, and B. Varghese

Department of Chemistry, Indian Institute of Technology—Madras, Chennai-600 036, India

Received November 27, 2005

To examine the influence of mixed substituents on the structural, electrochemical redox behavior of porphyrins, two new classes of β-pyrrole mixed substituted free-base tetraphenylporphyrins $H_2(TPP(Ph)_4X_4)$ (X = CH_3, H, Br, Cl, CN) and $H_2(TPP(CH_3)_4X_4)$ (X = H, Ph, Br, CN) and their metal (M = Ni(II), Cu(II), and Zn(II)) complexes have been synthesized effectively using the modified Suzuki cross-coupling reactions. Optical absorption spectra of these porphyrins showed significant red-shift with the variation of X in $H_2(TPPR_4X_4)$, and they induce a 20–30 nm shift in the B band and a 25–100 nm shift in the longest wavelength band [$Q_x(0,0)$] relative to the corresponding H_2TPPR_4 (R = CH_3, Ph) derivatives. Crystal structure of a highly sterically crowded $Cu(TPP(Ph)_4(CH_3)_4)\cdot 2CHCl_3$ complex shows a combination of ruffling and saddling of the porphyrin core while the $Zn(TPP(Ph)_4Br_4(CH_3OH))\cdot CH_3OH$ structure exhibits predominantly saddling of the macrocycle. Further, the six-coordinated $Ni(TPP(Ph)_4(CN)_4(Py)_2)\cdot 2(Py)$ structure shows nearly planar geometry of the porphyrin ring with the expansion of the core. Electrochemical redox behavior of the $MTPPR_4X_4$ compounds exhibit dramatic cathodic shift in first ring oxidation potentials (300–500 mV) while the reduction potentials are marginally cathodic in contrast to their corresponding $MTPPX_4$ (X = Br, CN) derivatives. The redox potentials were analyzed using Hammett plots, and the highest occupied molecular orbital–lowest unoccupied molecular orbital (HOMO–LUMO) gap decreases with an increase in the Hammett parameter of the substituents. Electronic absorption spectral bands of $H_2TPPR_4X_4$ are unique that their energy lies intermediate to their corresponding data for the $H_2(TPPX_8)$ (X = CH_3, Ph, Br, Cl) derivatives. The dramatic variation in redox potentials and large red-shift in the absorption bands in mixed substituted porphyrins have been explained on the basis of the nonplanarity of the macrocycle and substituent effects.

Introduction

Over the past 2 decades, considerable progress has been made on the synthesis of highly substituted porphyrins and their use as model compounds of nonplanar conformations of metalloporphyrinoids in nature.[1−9] Such nonplanar conformations of the porphyrin macrocycle arise from repulsive interactions among the peripheral substituents. The introduction of halogens at the peripheral positions of the high-valent metalloporphyrins provides robust catalysts for the oxidative transformation of organic substrates in the presence of strong oxygen donors to enhance cytochrome P450 like activity.[10−16] The robust nature of these perhaloporphyrin catalysts has

* To whom correspondence should be addressed. E-mail: bhyrappa@iitm.ac.in. Fax: 091-44-2257-0509.

(1) Shelnutt, J. A.; Song, X.-Z.; Ma, J.-G.; Jia, S.-L.; Jentzen, W.; Medforth, C. J. *Chem. Soc. Rev*. **1998**, *27*, 31 and references therein.
(2) Renner, M. W.; Furenlid, L. R.; Barkigia, K. M.; Forman, A.; Shim, H.-K.; Smith, K. M.; Fajer, J. *J. Am. Chem. Soc.* **1991**, *113*, 6891.
(3) Furenlid, L. R.; Renner, M. W.; Fajer, J. *J. Am. Chem. Soc*. **1990**, *112*, 8987.
(4) Barkigia, K. M.; Renner, M. W.; Furenlid, L. R.; Medforth, C. J.; Smith, K. M.; Fajer, J. *J. Am. Chem. Soc*. **1993**, *115*, 3627.
(5) Sparks, L. D.; Medforth, C. J.; Park, M.-S.; Chamberlain, J. R.; Ondrias, M. R.; Senge, M. O.; Smith, K. M.; Shelnutt, J. A. *J. Am. Chem. Soc*. **1993**, *115*, 581.
(6) Shelnutt, J. A.; Medforth, C. J.; Berber, M. D.; Barkigia, K. M.; Smith, K. M. *J. Am. Chem. Soc*. **1991**, *113*, 4077.
(7) Senge, M. O.; Medforth, C. J.; Sparks, L. D.; Shelnutt, J. A.; Smith, K. M. *Inorg. Chem*. **1993**, *32*, 1716.
(8) Renner, M. W.; Barkigia, K. M.; Zhang, Y.; Medforth, C. J.; Smith, K. M.; Fajer, *J. Am. Chem. Soc*. **1994**, *116*, 8582.
(9) Ravikanth, M.; Chandrashekar, T. K. *Struct. Bonding (Berlin)* **1995**, *82*, 105.
(10) Dolphin, D.; Traylor, T. G.; Xie, L. Y. *Acc. Chem. Res.* **1997**, *30*, 251 and references therein.
(11) Sheldon, R. A. *Metalloporphyrins in Catalytic Oxidations;* Marcel Dekker: New York, 1994.
(12) Montanari, F.; Casella, L. *Metalloporphyrins in Catalysed Oxidations;* Kluwer Academic Publishers: Dordrecht, The Netherlands, 1994.
(13) Grinstaff, M. W.; Hill, M. G.; Labinger, L. A.; Gray, H. B. *Science* **1994**, *264*, 1311.
(14) Meunier, B. *Chem. Rev*. **1992**, *92*, 1411.
(15) Ellis, P. E., Jr.; Lyons, J. E. *Coord. Chem. Rev*. **1990**, *105*, 181.
(16) Traylor, T. G.; Tsuchiya, S. *Inorg. Chem*. **1987**, *26*, 1338.

10.1021/ic052035b CCC: $33.50
Published on Web 04/22/2006

been attributed to the stabilization of the highest occupied π-molecular orbitals induced by the presence of halogen substituents.[16,17] Furthermore, these highly substituted porphyrins exhibit unique physicochemical properties.[1,18]

Of the synthetic porphyrin analogues, *meso*-tetraphenylporphyrin (TPP) is the most widely explored system because of its ease of synthesis and facile functionalization. M(TPP) complexes with similar β-octa-substituents (alkyl or phenyl)[2−8,18−21] and halogens[15,18,22−37] at the β-pyrrole and/or *meso*-phenyl positions have been reported in the literature. Electrochemical redox properties of M(TPP) complexes bearing fewer β-pyrrole substituents have been examined by various groups.[38−43] Kadish et al.[44−46] and others[8,24,25,27,47] have reported electrochemical redox properties of a variety of M(TPP) complexes bearing similar β-octa-substituents. Previous reports have shown that the number of β-substituents and the nonplanarity of the macrocycle influence the redox properties of the π-system.[17,48] Syntheses and properties of M(TPP) complexes with mixed antipodal β-octa-substituents have been largely unexamined.[49−51] In an effort to elucidate the role of mixed substituents at the antipodal β-pyrrole positions, we have synthesized two new classes of M(TPPR$_4$X$_4$) complexes (Figure 1) and explored their physicochemical properties. These porphyrins display interesting structural and electrochemical redox properties.

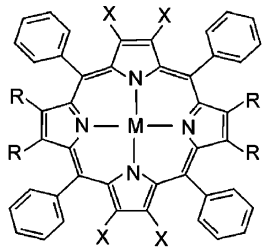

M = 2H, Ni(II), Cu(II), Zn(II)
R = Ph, X = H, CH_3, Br, Cl, CN
R = CH_3, X = H, Ph, Br, CN

Figure 1. Molecular structure of mixed substituted porphyrins and their metal complexes.

Experimental Section

Materials. 5,10,15,20-Tetraphenylporphyrin, H_2(TPP), its metal [Ni(II), Cu(II), Zn(II)] complexes,[52,53] and 2,3,12,13-tetrabromo-5,10,15,20-tetraphenylporphyrin,[54] H_2TPPBr$_4$, were synthesized using the literature methods.

All the solvents procured were of analytical grade and purified prior to use.[55] *N*-Bromosuccinimide (NBS) was recrystallized from hot water and dried at 60 °C under vacuum (2.0 mbar) for 12 h before use. *N*-Chlorosuccinimide (NCS) obtained from Aldrich was recrystallized from benzene and dried at 60 °C under vacuum (2.0 mbar) for 10 h. Calcium hydride, $CDCl_3$, benzene-d_6, superbase (2,8,9-triisobutyl-2,5,8,9-tetraaza-1-phosphabicyclo[3.3.3]-undecane), phenylboronic acid, methylboronic acid, tetrakis(triphenylphosphine)palladium(0), and cuprous cyanide were purchased from Sigma-Aldrich (India) and used as received. Metal acetates, copper(II) acetate monohydrate, zinc(II) acetate dihydrate, and nickel(II) acetate tetrahydrate were procured from Sigma-Aldrich (India) and used without further purification. Silica gel (60−120 mesh) and alumina (neutral and basic) for column chromatography

(17) D'Souza, F.; Zandler, M.; Tagliatesta, P.; Ou, Z.; Shao, J.; Van Caemelbecke, E.; Kadish, K. M. *Inorg. Chem.* **1998**, *37*, 4567.
(18) Senge, M. O. In *The Porphyrin Handbook;* Kadish, K. M., Smith, K. M., Guilard, R., Eds.; Academic Press: New York, 2000; Vol. 1, p 239 and references therein.
(19) Dolphin, D. *J. Heterocycl. Chem.* **1970**, *7*, 275.
(20) Evans, B.; Smith, K. M.; Fuhrhop, J.-H. *Tetrahedron Lett.* **1977**, *5*, 443.
(21) Ono, N.; Muratani, E.; Fumoto, Y.; Ogawa, T.; Tajima, K. *J. Chem. Soc., Perkin Trans. 1* **1998**, 3819.
(22) Hoffmann, P.; Labat, G.; Robert, A.; Meunier, B. *Tetrahedron Lett.* **1990**, *31*, 1991.
(23) Lyons, J. E.; Ellis, P. E. *Catal. Lett.* **1991**, *8*, 45.
(24) Wijesekara, T. P.; Matsumoto, A.; Dolphin, D.; Lexa, D. *Angew. Chem., Int. Ed. Engl.* **1990**, *29*, 1028.
(25) Bhyrappa, P.; Krishnan, V. *Inorg. Chem.* **1991**, *30*, 239.
(26) Mandon, D.; Ochsenbein, P.; Fischer, J.; Weiss, R.; Jayaraj, K.; Austin, R. N.; Gold, A.; White, P. S.; Brigaud, O.; Battioni, P.; Mansuy, D. *Inorg. Chem.* **1992**, *31*, 2044.
(27) DiMagno, S. G.; Williams, R. A.; Therien, M. J. *J. Org. Chem.* **1994**, *59*, 6943.
(28) Chorghade, M. S.; Dolphin, D.; Dupre, D.; Hill, D. R.; Lee, E. C.; Wijesekera, T. P. *Synthesis* **1996**, 1320.
(29) Bhyrappa, P.; Bhavana, P.; Vittal, J. J. *J. Porphyrins Phthalocyanines* **2003**, *7*, 682.
(30) Woller, E. K.; DiMagno, S. G. *J. Org. Chem.* **1997**, *62*, 1588.
(31) Leroy, J.; Bondon, A.; Toupet, L.; Rolando, C. *Chem.—Eur. J.* **1997**, *3*, 1890.
(32) Ono, N.; Kawamura, H.; Maruyama, K. *Bull. Chem. Soc. Jpn.* **1989**, *62*, 3386.
(33) Goll, J. G.; Moore, K. T.; Ghosh, A.; Therien, M. J. *J. Am. Chem. Soc.* **1996**, *118*, 8344.
(34) Ozette, K.; Leduc, P.; Palacio, M.; Bartoli, J.-F.; Barkigia, K. M.; Fajer, J.; Battioni, P.; Mansuay, D. *J. Am. Chem. Soc.* **1997**, *119*, 6442.
(35) Aoyagi, K.; Haga, T.; Toi, H.; Aoyama, Y.; Mizutani, T.; Ogoshi, H. *Bull. Chem. Soc. Jpn.* **1997**, *70*, 937.
(36) Tamaiki, H.; Nagata, Y.; Tsudzuki, S. *Eur. J. Org. Chem.* **1999**, 2471.
(37) Palacio, M.; Mansuy-Mauries, V.; Loire, G.; Le Branch-Ozette, K.; Ledue, P.; Barkigia, K. M.; Fajer, J.; Battioni, P.; Mansuy, D. *Chem. Commun.* **2000**, 1907.
(38) Giraudeau, A.; Callot, H. J.; Jordan, J.; Ezhar, I.; Gross, M. *J. Am. Chem. Soc.* **1979**, *101*, 3857.
(39) Giraudeau, A.; Callot, H. J.; Gross, M. *Inorg. Chem.* **1979**, *18*, 201.
(40) Giraudeau, A.; Louati, A.; Callot, H. J.; Gross, M. *Inorg. Chem.* **1981**, *20*, 769.
(41) Binstead, R. A.; Crossley, M. J.; Hush, N. S. *Inorg. Chem.* **1991**, *30*, 1259.
(42) (a) Terazono, Y.; Patrick, B. O.; Dolphin, D. *Inorg. Chem.* **2002**, *41*, 6703. (b) Terazono, Y.; Dolphin, D. *J. Org. Chem.* **2003**, *68*, 1892.
(43) Kadish, K. M.; Royal, G.; Caemelbecke, E. V.; Gueletti, L. In *The Porphyrin Handbook;* Kadish, K. M., Smith, K. M., Guilard, R., Eds.; Academic Press: New York, 2000; Vol. 9, p 59 and references therein.
(44) Kadish, K. M.; D'Souza, F.; Villard, A.; Autret, M.; Van Caemelbecke, E.; Bianco, P.; Antonio, A.; Tagliatesta, P. *Inorg. Chem.* **1994**, *33*, 5169.
(45) D'Souza, F.; Villard, A.; Van Caemelbecke, E.; Franzen, M. M.; Boschi, T.; Tagliatesta, P.; Kadish, K. M. *Inorg. Chem.* **1993**, *32*, 4042.
(46) Kadish, K. M.; Van Caemelbecke, E.; Boulas, P.; D'Souza, F.; Vogel, E.; Kisters, M.; Medforth, C. J.; Smith, K. M. *Inorg. Chem.* **1993**, *32*, 4177.
(47) Takeda, M.; Sato, M. *Chem. Lett.* **1995**, 939.
(48) Ochsenbein, P.; Ayougou, K.; Mandon, D.; Fischer, J.; Weiss, R.; Austin, R. N.; Jayaraj, K.; Gold, A.; Terner, J.; Fajer, J. *Angew. Chem., Int. Ed. Engl.* **1994**, *33*, 348.
(49) Senge, M. O.; Gerstung, V.; Ruhlandt-Senge, K.; Runge, S.; Lehmann, I. *J. Chem. Soc., Dalton Trans.* **1998**, 4187.
(50) Duval, H.; Bulach, V.; Fischer, J.; Weiss, R. *Inorg. Chem.* **1999**, *38*, 5495.
(51) Leroy, J.; Porhiel, E.; Bondon, A. *Tetrahedron* **2002**, *58*, 6713.
(52) Lindsey, J. S.; Wagner, R. W. *J. Org. Chem.* **1989**, *54*, 828.
(53) Adler, A. D.; Longo, F. R.; Kampas, F.; Kim, J. *J. Inorg. Nucl. Chem.* **1970**, *32*, 2443.
(54) Kumar, P. K.; Bhyrappa, P.; Varghese, B. *Tetrahedron Lett.* **2003**, *44*, 4849.
(55) Armarego, W. L. F.; Chai, C. L. L. *Purification of Laboratory Chemicals;* Elsevier: New York, 2003.

procured from Acmes (India) were used as such. Precoated thin-layer silica gel chromatography and aluminum plates were purchased from E. Merck (Germany) and used as received. Tetrabutylammonium hexafluorophosphate, $TBAPF_6$, procured from Fluka (Switzerland) was recrystallized thrice from absolute ethanol and stored in a vacuum desiccator.

Instrumentation and Methods. Electronic absorption spectra of porphyrins and their metal complexes were performed on a computer interfaced JASCO V-550 model UV−visible spectrophotometer using a pair of quartz cells of 10 mm path length in CH_2Cl_2 at 298 K. ^1H NMR spectra of porphyrins were recorded on a Bruker Avance 400 MHz FT-NMR spectrometer in $CDCl_3$ using tetramethylsilane as the internal reference. Mass spectral measurements of the samples were carried out using electrospray ionization (ESI) mass spectrometer model Micromass Q-TOF Micro using 10% formic acid in methanol as the solvent medium. Low-resolution fast atom bombardment mass spectra (FAB-MS) of the samples were obtained on a JEOL SX 102/DA-6000 model using *m*-nitrobenzyl alcohol as the matrix. In some cases, a matrix assisted laser desorption time-of-flight (MALDI-TOF) spectrum on a Voyager DE-PRO model mass spectrometer was used by employing α-cyano-4-hydroxycinnamic acid as the matrix. Elemental analysis of the samples was performed on a Perkin-Elmer CHNO/S analyzer model 2400 series. Cyclic voltammetric measurements of the porphyrins were taken on a CH instruments model 660B or Bioanalytical Systems model BAS-100A. The electrochemical cell consists of a three-electrode cell assembly: a platinum button as a working electrode, Ag/AgCl as a reference electrode, and platinum wire as the counter electrode. The concentrations of all the porphyrins employed were 0.5−1.0 mM, and 0.1 M tetrabutylammonium hexafluorophosphate, $TBAPF_6$, was used as the supporting electrolyte. All cyclic voltammetric measurements were performed in triply distilled CH_2Cl_2 from CaH_2 and stored over 4 Å molecular sieves.

Crystal Structures. Mixed substituted porphyrins $Cu(TPP(Ph)_4(CH_3)_4)$ and $Zn(TPP(Ph)_4Br_4)$ were crystallized by direct diffusion of CH_3OH to a saturated porphyrin solution in $CHCl_3$ over a period of 7 days. Crystals of the $NiTPP(Ph)_4(CN)_4$ complex were obtained by slow diffusion of hexane to the saturated porphyrin solution in pyridine. X-ray diffraction data were collected on Enraf-Nonius CAD-4 diffractometer at 293 K. Cell refinement was done with the CAD4 system software, data reduction with XCAD4 (wingx). Twenty-five reflections, collected through a search routine from different zones of the crystal, were indexed using a method of short vectors followed by least-squares refinement. Intensity data from one quadrant of the reciprocal space were collected. The systematic absences clearly revealed the space groups. The intensity data were corrected for background, Lorentz, polarization, and decay corrections. Empirical absorption corrections using ψ-scan data were used for absorption. A total of $I > 2\sigma(I)$ reflections were taken for structure solution. The SIR92 (WINGX) program was used to solve the structure by direct methods. Successive Fourier synthesis was employed to complete the structures. The structure was refined with a full matrix least-squares technique on F^2 using SHELXL97 software (Sheldrik, 1997).[56] Non-hydrogen atoms were refined with anisotropic thermal parameters. The positions of hydrogen atoms were assigned geometrically and were given riding model refinement. In the case of the $ZnTPP(Ph)_4Br_4$ structure, the bromine atoms and the coordinated methanol were found to have some positional disorder. The disordered positions were located from a difference Fourier map. Refinement of disordered atoms were carried out with their relative occupancies as least-squares variables. However, the sum of the occupancies of disordered pairs was constrained to be 1.0. Complete bond lengths, bond angles, and isotropic thermal parameters for all the three crystal structures examined in this work are given in the Supporting Information.

I. Synthesis of Mixed Substituted Tetraphenylporphyrin, $M(TPP(Ph)_4X_4)$ Derivatives. (a) 2,3,12,13-Tetraphenyl-5,10,15,-20-tetraphenylporphyrin ($H_2(TPP(Ph)_4)$) and Its Metal Complexes. 2,3,12,13-Tetraphenyl-5,10,15,20-tetraphenylporphyrin ($H_2(TPP(Ph)_4)$) was synthesized using a modified Suzuki cross-coupling reaction,[57,58] and its metal [Ni(II), Cu(II), and Zn(II)] complexes were prepared by conventional procedures.[53,25]

The two-way stoppered round-bottom flask (250 mL) containing freshly distilled toluene from metallic sodium (170 mL) was charged with $H_2(TPPBr_4)$ (0.93 g, 1.0 mmol), tetrakis(triphenylphosphine)-palladium(0) (20 mol %, 0.232 g), 2,8,9-triisobutyl-2,5,8,9-tetraaza-1-phosphabicyclo[3.3.3]undecane (0.070 mL, 0.20 mmol), anhydrous K_2CO_3 (3.32 g, 24.0 mmol), and phenylboronic acid (1.45 g, 12.0 mmol) and degassed by the freeze−pump−thaw method (three cycles). Then the suspension was heated and stirred between 95 and 105 °C under N_2 atmosphere for 2 days. After completion of the reaction, toluene was removed by rotary evaporation under reduced pressure. The crude product was redissolved in $CHCl_3$ and washed with saturated aqueous $NaHCO_3$ solution (100 mL) followed by 30% aqueous NaCl solution (100 mL). Then, the organic layer was dried over anhydrous Na_2SO_4. The concentrated solution of the crude product was chromatographed on a silica column using $CHCl_3$ as the eluent. Trace amounts of the hydrogenated porphyrin product were eluted first followed by the desired $H_2(TPP(Ph)_4)$ as the major product. The product was recrystallized from $CHCl_3/CH_3OH$ (1:3, v/v) solvent mixture and dried under vacuum (3 mbar) at 100 °C for 5 h. The yield of the product was found to be 0.78 g (85%). $H_2(TPP(Ph)_4)$ ^1H NMR in $CDCl_3$ δ (ppm): 8.30 (s, 4H, β-pyrrole-H), 7.76 (d, 8H, *meso-o*-phenyl-H), 7.16 (m, 12H, *meso-m*- and *p*-phenyl-H), 6.81 (m, 20H, β-pyrrole-phenyl-H), −2.13 (s, 2H, imino-H). FAB-MS (*m*/*z*): 919 (calcd, 919.14).

The metal [Ni(II), Cu(II), and Zn(II)] complexes of $H_2(TPP(Ph)_4)$ were prepared almost in excellent (80−90%) yields using conventional procedures.[25] $Ni(TPP(Ph)_4)$ ^1H NMR in $CDCl_3$: 8.11 (s, 4H, β-pyrrole-H), 7.37 (d, 8H, *meso-o*-phenyl-H), 7.07 (t, 4H, *meso-p*-phenyl-H), 6.97 (t, 8H, *meso-m*-phenyl-H), 6.76 (m, 20H, β-pyrrole-phenyl-H). FAB-MS (*m*/*z*): 975 (calcd, 975.81). $Cu(TPP(Ph)_4)$ FAB-MS (*m*/*z*): 980 (calcd, 980.67). $Zn(TPP(Ph)_4)$ ^1H NMR in $CDCl_3$: 8.42 (s, 4H, β-pyrrole-H), 7.69 (d, 8H, *meso-o*-phenyl-H), 7.15 (t, 4H, *meso-p*-phenyl-H), 7.08 (t, 8H, *meso-m*-phenyl-H), 6.88 (d, 8H, β-pyrrole-*o*-phenyl-H), 6.75 (m, 12H, β-pyrrole-*m*- and *p*-phenyl-H). FAB-MS (*m*/*z*): 982 (calcd, 982.5).

(b) Preparation of 2,3,12,13-Tetrabromo-7,8,17,18-tetraphenyl-5,10,15,20-tetraphenylporphyrin ($H_2(TPP(Ph)_4Br_4)$) and Its Metal Complexes. The mixed substitution at the β-pyrrole positions of the $H_2(TPP)$ was effected by the bromination of $Ni(TPP(Ph)_4)$ with *N*-bromosuccinimide in refluxing $CHCl_3$ to produce the corresponding $Ni(TPP(Ph)_4Br_4)$ complex. Its free-base porphyrin ($H_2(TPP(Ph)_4Br_4)$) was obtained by acid demetalation reaction of the $NiTPP(Ph)_4Br_4$ complex. Other $M(TPP(Ph)_4Br_4)$ [M = Cu(II)

(56) Sheldrick, G. M. *SHELXL*97, *Program for the Refinement of Crystal Structures*; University of Göettingen: Göettingen, Germany, 1997.

(57) (a) Chan, K. S.; Zhou, X.; Lou, B.-S.; Mak, T. C. W. *J. Chem. Soc., Chem. Commun.* **1994**, 271. (b) Chan, C.-S.; Tse, K.-S.; Chan, K. S. *J. Org. Chem.* **1996**, *59*, 6084. (c) Chan, K. S.; Zhou, X.; Au, M. T.; Tam, C. Y. *Tetrahedron* **1995**, *51*, 3129.

(58) Urgaonkar, S.; Nagarajan, M.; Verkade, J. G. *Tetrahedron Lett.* **2002**, *43*, 8921.

and Zn(II)] complexes were prepared using their appropriate metal-(II) acetates as metal carriers as described in the literature.[25,53]

Ni(TPP(Ph)$_4$) (0.38 g, 0.39 mmol) was dissolved in $CHCl_3$ (50 mL). To this solution, freshly recrystallized NBS (0.416 g, 2.34 mmol) was added. The reaction mixture was refluxed for 4 h and cooled to room temperature, and the $CHCl_3$ was removed by rotary evaporation. The residue thus obtained was washed with methanol (2 × 10 mL) to remove any soluble succinimide and degraded porphyrin impurities. Then the greenish-purple colored product was chromatographed on a silica column using $CHCl_3$ as the eluent. The first fraction was collected, and chloroform was removed to obtain the Ni(TPP(Ph)$_4$Br$_4$) complex. This was dried for 6 h under vacuum (3 mbar) at 100 °C, and the yield of Ni(TPP(Ph)$_4$Br$_4$) was 0.46 g (90%). Ni(TPP(Ph)$_4$Br$_4$) ^{1}H NMR in benzene-d_6: 7.50 (d, 8H, *meso*-*o*-phenyl-H), 7.06 (t, 4H, *meso*-*p*-phenyl-H), 6.99 (t, 8H, *meso*-*m*-phenyl-H), 6.76 (d, 8H, β-pyrrole-*o*-phenyl-H), 6.64 (m, 12H, β-pyrrole-*m*- and *p*-phenyl-H). FAB-MS (*m*/*z*): 1291 (calcd, 1291.4). Anal. Calcd for $C_{68}H_{40}N_4Br_4Ni$: C, 63.25; H, 3.12; N, 4.34%. Found: C, 63.25; H, 3.12; N, 4.32%.

Preparation of H$_2$(TPP(Ph)$_4$Br$_4$). Ni(TPP(Ph)$_4$Br$_4$) (0.30 g, 0.23 mmol) was dissolved in a minimum amount of chloroform. To this, concentrated H_2SO_4 (2.0 mL) was added, and the solution was stirred for 45 min at 0 °C. At the end of this period, distilled water (100 mL) was added dropwise to the reaction mixture with stirring. The organic layer was separated and washed with water (2 × 50 mL) followed by neutralization using aqueous ammonia (25%) solution (20 mL). Then the organic layer was dried over anhydrous Na_2SO_4 and concentrated to a small volume. This was separated by silica gel chromatography using $CHCl_3$ as the eluent, and the yield of the product was found to be 0.26 g (90%).

The metal complexes of the H$_2$(TPP(Ph)$_4$Br$_4$) derivative were prepared using the reported methods,[25] and the yields of the products were 85−95%. H$_2$(TPP(Ph)$_4$Br$_4$) ^{1}H NMR in $CDCl_3$: 7.85 (d, 8H, *meso*-*o*-phenyl-H), 7.23 (m, 12H, *meso*-*m*- and *p*-phenyl-H), 6.75 (m, 20H, β-pyrrole-phenyl-H), −1.79 (bs, 2H, imino-H). FAB-MS (*m*/*z*): 1235 (calcd, 1234.72). Cu(TPP(Ph)$_4$Br$_4$) FAB-MS (*m*/*z*): 1297 (calcd, 1296.25). Zn(TPP(Ph)$_4$Br$_4$) ^{1}H NMR in $CDCl_3$: 7.86 (d, 8H, *meso*-*o*-phenyl-H), 7.25 (m, 12H, *meso*-*m*- and *p*-phenyl-H), 6.77 (m, 20H, β-pyrrole phenyl-H). FAB-MS (*m*/*z*): 1297 (calcd, 1298.09).

(c) 2,3,12,13-Tetrachloro-7,8,17,18-tetraphenyl-5,10,15,20-tetraphenylporphyrin (H$_2$(TPP(Ph$_4$)Cl$_4$)) and Its Metal Complexes. Ni(TPP(Ph)$_4$) (0.18 g, 0.184 mM) was dissolved in 1,1,2,2-tetrachloroethane (30 mL). To this, freshly recrystallized *N*-chlorosuccinimide (0.197 g, 1.47 mM) in TCE (20 mL) was added, and the resulting solution was refluxed for 3 h under argon atmosphere. After completion of the reaction, the solvent was removed by rotary evaporation. The residue thus obtained was washed with methanol to remove any soluble succinimide impurities. Then the crude product Ni(TPP(Ph$_4$)Cl$_4$) was chromatographed on a silica gel column using chloroform as eluent. The yield of the product was 0.19 g (92%). Ni(TPP(Ph)$_4$Cl$_4$) ^{1}H NMR in $CDCl_3$: 7.42 (d, 8H, *meso*-*o*-phenyl-H), 7.18 (t, 4H, *meso*-*p*-phenyl-H), 7.04 (t, 8H, *meso*-*m*-phenyl-H), 6.78 (d, 8H, β-pyrrole-*o*-phenyl-H), 6.69 (m, 12H, β-pyrrole-*m*- and *p*-phenyl-H). MALDI-TOF-MS (*m*/*z*): 1113.05 (calcd, 1113.59). Anal. Calcd for $C_{68}H_{40}N_4Cl_4Ni$: C, 73.34; H, 3.62; N, 5.03%. Found: C, 73.34; H, 3.50; N, 5.30%.

H$_2$(TPP(Ph)$_4$Cl$_4$) and its metal [Cu(II) and Zn(II)] complexes were prepared as described above for the synthesis of M(TPP-(Ph)$_4$Br$_4$) [M = 2H, Cu(II), and Zn(II)] derivatives. The yields of the products were almost quantitative. H$_2$(TPP(Ph)$_4$Cl$_4$) ^{1}H NMR in $CDCl_3$: 7.93 (d, 8H, *meso*-*o*-phenyl-H), 7.31 (m, 12H, *meso*-*m*- and *p*-phenyl-H), 6.89 (m, 20H, β-pyrrole-phenyl-H), −1.80 (bs, 2H, imino-H). ESI-MS (*m*/*z*): 1057 (calcd, 1056.92). Zn(TPP-(Ph)$_4$Cl$_4$) ^{1}H NMR in $CDCl_3$: 7.67 (d, 8H, *meso*-*o*-phenyl-H), 7.15 (m, 12H, *meso*-*m*- and *p*-phenyl-H), 6.69 (m, 20H, β-pyrrole phenyl-H). MALDI-TOF-MS (*m*/*z*): 1119.10 (calcd, 1120.28). Cu(TPP-(Ph)$_4$Cl$_4$): MALDI-TOF-MS (*m*/*z*): 1117.12 (calcd, 1118.54).

(d) 2,3,12,13-Tetramethyl-7,8,17,18-tetraphenyl-5,10,15,20-tetraphenylporphyrin (H$_2$(TPP(Ph)$_4$(CH$_3$)$_4$)) and Its Metal Complexes. To a 250 mL two necked round-bottom flask containing H$_2$TPP(Ph)$_4$Br$_4$ (0.106 g, 0.085 mmol) in toluene (15 mL), Pd-(PPh$_3$)$_4$ (20 mol %, 0.02 g), anhydrous K_2CO_3 (0.381 g, 2.70 mmol), and methylboronic acid (0.083 g, 1.38 mmol) in dry THF (5 mL) were added. The reaction mixture was degassed by the freeze−pump−thaw method (three cycles), and it was stirred and maintained between 85 and 95 °C under N_2 atmosphere for 3 days. After completion of reaction, the solvent was evaporated to dryness. The crude product was redissolved in $CHCl_3$ and washed with saturated aqueous $NaHCO_3$ (25 mL) solution followed by saturated aqueous NaCl (30 mL) solution, and the organic layer was dried over anhydrous Na_2SO_4. The solution was concentrated and loaded on a silica gel column, and trace amounts of hydrogenated porphyrin product were eluted first with $CHCl_3$. Then the required product H$_2$(TPP(Ph)$_4$(CH$_3$)$_4$) was eluted as a second fraction using 4% acetone in $CHCl_3$. The product was recrystallized from a $CHCl_3$/CH_3OH (4:1, v/v) mixture and dried under vacuum (2 mbar) at 90 °C for a period of 6 h. The yield of the product was 0.055 g (65%). The metal complexes of the H$_2$(TPP(Ph)$_4$(CH$_3$)$_4$) derivative were prepared using conventional procedures as described above. In all these reactions, the yields were 85−90%. H$_2$(TPP(Ph)$_4$(CH$_3$)$_4$) ^{1}H NMR in $CDCl_3$: 7.92 (d, 8H, *meso*-*o*-phenyl-H), 7.56 (t, 4H, *meso*-*p*-phenyl-H), 7.46 (t, 8H, *meso*-*m*-phenyl-H), 6.74 (m, 20H, β-pyrrole-phenyl-H), 1.82 (s, 12H, β-pyrrole-methyl-H), −1.65 (bs, 2H, imino-H). ESI-MS (*m*/*z*): 974.83 (calcd, 975.25). Anal. Calcd for $C_{72}H_{54}N_4$: C, 88.67; H, 5.58; N, 5.74%. Found: C, 88.37; H, 5.49; N, 5.57%. Ni(TPP(Ph)$_4$(CH$_3$)$_4$) ^{1}H NMR in $CDCl_3$: 7.48 (d, 8H, *meso*-*o*-phenyl-H), 7.10 (t, 4H, *meso*-*p*-phenyl-H), 7.02 (t, 8H, *meso*-*m*-phenyl-H), 6.68 (m, 20H, β-pyrrole-phenyl-H), 1.58 (s, 12H, β-pyrrole-methyl-H). ESI-MS (*m*/*z*): 1030.68 (calcd, 1031.92). Cu(TPP(Ph)$_4$(CH$_3$)$_4$) MALDI-TOF-MS (*m*/*z*): 1036.09 (calcd, 1036.78). Zn(TPP(Ph)$_4$(CH$_3$)$_4$) ^{1}H NMR in $CDCl_3$: 7.74 (d, 8H, *meso*-*o*-phenyl-H), 7.15 (m, 12H, *meso*-*m*- and *p*-phenyl-H), 6.68 (m, 20H, β-pyrrole-phenyl-H), 1.72 (s, 12H, β-pyrrole-methyl-H). LD-MS (*m*/*z*): 1038.20 (calcd, 1038.61).

(e) 2,3,12,13-Tetracyano-7,8,17,18-tetraphenyl-5,10,15,20-tetraphenylporphyrin (H$_2$(TPP(Ph)$_4$(CN)$_4$)) and Its Metal Complexes. H$_2$(TPP(Ph)$_4$(CN)$_4$) was obtained by the direct cyanation of Ni(TPP(Ph)$_4$Br$_4$) complex by using a variation of the reported procedure[59] followed by an acid demetalation reaction. The typical procedure is as follows: Ni(TPP(Ph)$_4$Br$_4$) (0.151 g, 0.117 mmol) was dissolved in dry pyridine (30 mL). To this, CuCN (0.42 g, 4.69 mmol) was added in the solid form. Then the reaction mixture was stirred and refluxed for a period of 48 h under argon atmosphere. At the end of this period, the solvent was rotary evaporated under reduced pressure. Further, the resultant residue was redissolved in a minimum amount of $CHCl_3$, and it was loaded onto a silica gel column using $CHCl_3$ as the eluent. The first fraction [Ni(TPP(Ph)$_4$(CN)$_3$)] was found to be 0.025 g (20%). The desired product [Ni(TPP(Ph$_4$)(CN)$_4$)] was eluted as the second fraction (0.070 g, 56%). Ni(TPP(Ph$_4$)(CN)$_3$) ^{1}H NMR in $CDCl_3$: 8.64 (s, 1H, β-pyrrole-H), 7.47−7.39 (m, 8H, *meso*-*o*-phenyl-H), 7.34−

(59) (a) Callot, H. J.; Giraudeau, A.; Gross, M. *J. Chem. Soc., Perkin Trans. 2* **1975**, 1321. (b) Callot, H. J. *Tetrahedron Lett.* **1973**, 4987. (c) Callot, H. J. *Bull. Soc. Chim. Fr.* **1974**, 1492.

7.00 (m, 12H, *meso*-*p*- and *m*-phenyl-H), 6.98−6.66 (m, 20H, β-pyrrole-phenyl-H). Electronic absorption spectrum in CH_2Cl_2, λ_{max}, nm (log ϵ): 329 (4.34), 451 (5.17), 537 (3.74), 576 (sh), 635 (4.31). MALDI-TOF-MS (*m*/*z*): 1051.9 (calcd, 1050.84). Ni(TPP-$(Ph)_4(CN)_4$) ^{1}H NMR in $CDCl_3$: 7.39 (d, 8H, *meso*-*o*-phenyl-H), 7.30 (t, 4H, *meso*-*p*-phenyl-H), 7.10 (t, 8H, *meso*-*m*-phenyl-H), 6.87 (t, 4H, β-pyrrole-*p*-phenyl-H), 6.78 (t, 8H, β-pyrrole-*m*-phenyl-H), 6.68 (d, 8H, β-pyrrole-*o*-phenyl-H). MALDI-TOF-MS (*m*/*z*): 1074.18 (calcd, 1075.85). Anal. Calcd for $C_{72}H_{40}N_8Ni$: C, 80.38; H, 3.75; N, 10.42%. Found: C, 80.10; H, 3.85; N, 10.14%.

The free-base porphyrin was prepared by acid demetalation reaction as described above, and the yield of the product was 85%. $H_2(TPP(Ph)_4(CN)_4)$ ^{1}H NMR in $CDCl_3$: 7.84 (d, 8H, *meso*-*o*-phenyl-H), 7.51 (t, 4H, *meso*-*p*-phenyl-H), 7.35 (t, 8H, *meso*-*m*-phenyl-H), 6.89 (m, 20H, β-pyrrole-phenyl-H), −1.48 (s, 2H, imino-H). MALDI-TOF-MS (*m*/*z*): 1019.22 (calcd, 1019.18). Metal complexes (Cu(II) and Zn(II)) of $H_2(TPP(Ph)_4(CN)_4)$ were prepared as described above. Yields are almost quantitative (85−95%). Cu-$(TPP(Ph)_4(CN)_4)$ MALDI-TOF-MS (*m*/*z*): 1079.71 (calcd, 1080.71). $Zn(TPP(Ph)_4(CN)_4)$ ^{1}H NMR in $CDCl_3$: 7.63 (d, 8H, *meso*-*o*-phenyl-H), 7.37 (t, 4H, *meso*-*p*-phenyl-H), 7.10 (t, 8H, *meso*-*m*-phenyl-H), 6.75 (m, 20H, β-pyrrole-phenyl-H). LD-MS (*m*/*z*): 1081.73 (calcd, 1082.54).

II. Synthesis of Mixed Substituted Tetraphenylporphyrins, M(TPP(CH$_3$)$_4$X$_4$) Derivatives. (a) 2,3,12,13-Tetramethyl-5,10,-15,20-tetraphenylporphyrin (H_2(TPP(CH$_3$)$_4$)) and Its Metal Complexes. The free-base porphyrin $H_2(TPP(CH_3)_4)$ was prepared using the reported procedure[57] or modified Suzuki cross-coupling reaction of $H_2(TPPBr_4)$ with methylboronic acid as described for the synthesis of the $H_2(TPP(Ph)_4)$ derivative. The product was separated on a basic alumina column using $CHCl_3$ as the eluent. The product was recrystallized from a $CHCl_3/CH_3OH$ (1:5, v/v) solvent mixture and dried under vacuum (3 mbar) at 90 °C over a period of 6 h. The yield of the product was found to be 90%. H_2-$(TPP(CH_3)_4)$ ^{1}H NMR in $CDCl_3$: 8.46 (s, 4H, β-pyrrole-H), 8.10 (d, 8H, *meso*-*o*-phenyl-H), 7.73 (m, 12H, *meso*-*m*- and *p*-phenyl-H), 2.45 (s, 12H, β-pyrrol*e*-methyl-H), −2.76 (s, 2H, imino-H). ESI-MS (*m*/*z*): 671.51 (calcd, 670.86). The $MTPP(CH_3)_4$ (M = Zn(II) and Cu(II)) complexes were prepared using a variation of literature methods.[25]

The $Ni(TPP(CH_3)_4)$ complex was prepared using the reported procedure[53] and its yield was 90%. $Ni(TPP(CH_3)_4)$ ^{1}H NMR in $CDCl_3$: 8.49 (s, 4H, β-pyrrole-H), 7.86 (d, 8H, *meso*-*o*-phenyl-H), 7.62 (m, 12H, *meso*-*m*- and *p*-phenyl-H), 2.16 (s, 12H, β-pyrrole-methyl-H). MALDI-TOF-MS (*m*/*z*): 727.41 (calcd, 727.53). $Cu(TPP(CH_3)_4)$ MALDI-TOF-MS (*m*/*z*): 732.56 (calcd, 732.39). $Zn(TPP(CH_3)_4)$ ^{1}H NMR in $CDCl_3$: 8.66 (s, 4H, β-pyrrole-H), 8.08 (d, 8H, *meso*-*o*-phenyl-H), 7.70 (m, 12H, *meso*-*m*- and *p*-phenyl-H), 2.37 (s, 12H, β-pyrrole-methyl-H). MALDI-TOF-MS (*m*/*z*): 734.08 (calcd, 734.22).

(b) 2,3,12,13-Tetrabromo-7,8,17,18-tetramethyl-5,10,15,20-tetraphenylporphyrin (H_2(TPP(CH$_3$)$_4$Br$_4$)) and Its Metal Complexes. The title porphyrin was obtained by bromination of the $Ni(TPP(CH_3)_4)$ complex followed by an acid demetalation reaction as given in the synthesis of the $H_2(TPP(Ph)_4Br_4)$ derivative. The yield of the product $Ni(TPP(CH_3)_4Br_4)$ was 75%. $Ni(TPP(CH_3)_4$-$Br_4)$ ^{1}H NMR in $CDCl_3$: 7.95 (d, 8H, *meso*-*o*-phenyl-H), 7.67 (m, 12H, *meso*-*m*- and *p*-phenyl-H), 1.79 (s, 12H, β-pyrrole-methyl-H). MALDI-TOF-MS (*m*/*z*): 1043.81 (calcd, 1043.11). Anal. Calcd for $C_{48}H_{32}N_4Br_4Ni$: C, 55.27; H, 3.09; N, 5.37%. Found: C, 55.19; H, 3.55; N, 5.18%.

The demetalation of the porphyrin $Ni(TPPBr_4(CH_3)_4)$ was performed as described above with 85% yield of $H_2(TPP(CH_3)_4$-$Br_4)$. The other metal complexes were prepared as described earlier. $H_2(TPP(CH_3)_4Br_4)$ ^{1}H NMR in $CDCl_3$: 8.26 (d, 8H, *meso*-*o*-phenyl-H), 7.78 (m, 12H, *meso*-*m*- and *p*-phenyl-H), 1.95 (s, 12H, β-pyrrole methyl-H), −2.25 (bs, 2H, imino-H). MALDI-TOF-MS (*m*/*z*): 987.25 (calcd, 986.44). $Cu(TPP(CH_3)_4Br_4$ MALDI-TOF-MS (*m*/*z*): 1048.39 (calcd, 1047.97). $Zn(TPP(CH_3)_4Br_4)$ ^{1}H NMR in $CDCl_3$: 8.14 (d, 8H, *meso*-*o*-phenyl-H), 7.74 (m, 12H, *meso*-*m*- and *p*-phenyl-H), 1.51 (s, 12H, β-pyrrole-methyl-H). MALDI-TOF-MS (*m*/*z*): 1053.0 (calcd, 1049.80).

(c) 2,3,12,13-Tetracyano-7,8,17,18-tetramethyl-5,10,15,20-tetraphenylporphyrin (H_2TPP(CH$_3$)$_4$(CN)$_4$) and Its Metal Complexes. $H_2(TPP(CH_3)_4(CN)_4)$ was prepared as described in the synthesis of the $Ni(TPP(Ph)_4(CN)_4)$ complex. The first fraction, $Ni(TPP(CH_3)_4(CN)_3)$, was found to be 15%. The product Ni(TPP-$(CH_3)_4(CN)_4$ was eluted as a second fraction in 40% yield. Ni-$(TPP(CH_3)_4(CN)_4)$ ^{1}H NMR in $CDCl_3$: 7.89 (d, 8H, *meso*-*o*-phenyl-H), 7.84 (t, 4H, *meso*-*p*-phenyl-H), 7.73 (t, 8H, *meso*-*m*-phenyl-H), 1.94 (s, 12H, β-pyrrole-methyl-H). MALDI-TOF-MS (*m*/*z*): 826.86 (calcd, 827.57). Anal. Calcd for $C_{52}H_{32}N_8Ni$: C, 75.47; H, 3.90; N, 13.54%. Found: C, 75.35; H, 3.77; N, 13.78%. Ni(TPP-$(CH_3)_4(CN)_3)$ ^{1}H NMR in $CDCl_3$: 8.86 (s, H, β-pyrrole-H), 7.91-(m, 8H, *meso*-*o*-phenyl-H), 7.89−7.65 (m, 12H, *meso*-*p*- and *m*-phenyl-H), 2.00−1.92 (m, 12H, β-pyrrole-methyl-H). UV−visible in CH_2Cl_2, λ_{max}, nm (log ϵ): 329 (4.16), 443 (5.05), 533 (3.60), 573 (sh), 633 (4.31). MALDI-TOF-MS (*m*/*z*): 802.26 (calcd, 802.56).

The free-base porphyrin was prepared by the demetalation of the $Ni(TPP(CH_3)_4(CN)_4)$ complex with sulfuric acid. The yield of the free-base porphyrin was 85%. $H_2(TPP(CH_3)_4(CN)_4)$ ^{1}H NMR in $CDCl_3$: 8.16 (d, 8H, *meso*-*o*-phenyl-H), 7.97 (t, 4H, *meso*-*p*-phenyl-H), 7.85 (t, 8H, *meso*-*m*-phenyl-H), 2.21 (s, 12H, β-pyrrole-methyl-H), −2.02 (s, 2H, imino-H). MALDI-TOF-MS (*m*/*z*): 771.31 (calcd, 770.90). $M(TPP(CH_3)_4(CN)_4)$ (M = Cu(II) and Zn-(II)) complexes were prepared using conventional procedures.[7] Yields were almost quantitative (85−95%). $Cu(TPP(CH_3)_4(CN)_4)$ MALDI-TOF-MS (*m*/*z*): 833.55 (calcd, 832.43). $Zn(TPP(CH_3)_4$-$(CN)_4)$ ^{1}H NMR in $CDCl_3$: 8.06 (d, 8H, *meso*-*o*-phenyl-H), 7.91 (t, 4H, *meso*-*p*-phenyl-H), 7.78 (t, 8H, *meso*-*m*-phenyl-H), 2.09 (s, 12H, β-pyrrole-methyl-H). MALDI-TOF-MS (*m*/*z*): 835.68 (calcd, 834.26).

Results and Discussion

Synthesis and Characterization. A series of antipodal β-pyrrole mixed substituted TPPs were synthesized using H_2-$(TPPBr_4)$ as the precursor. The synthetic route for the preparation of various antipodal substituted porphyrins is shown in Scheme 1. The choice of the brominated porphyrin for the preparation of mixed substituted porphyrins is due to the ease of synthesis and to its ability to provide entry to other groups at the other antipodal β-pyrrole positions. Recent reports show that Suzuki cross-coupling reactions for sterically hindered monobromoarenes using $Pd(OAc)_2$ as the catalyst with superbase in the presence of Cs_2CO_3 proceed in shorter time scales (<12 h).[58] This procedure was not feasible to convert the $H_2(TPPBr_4)$ to $H_2(TPP(Ph_4))$ even under a longer reaction time (3 days) and yielded a mixture of products. $H_2(TPP(Ph)_4)$ was synthesized in good yields using a modified Suzuki cross-coupling reaction of H_2-$(TPPBr_4)$ with phenylboronic acid in the presence of Pd(0) catalyst using superbase and K_2CO_3 in a toluene/THF medium over a period of 2 days. The observed spectral data

Scheme 1. Synthetic Route for Various Mixed Substituted Porphyrins

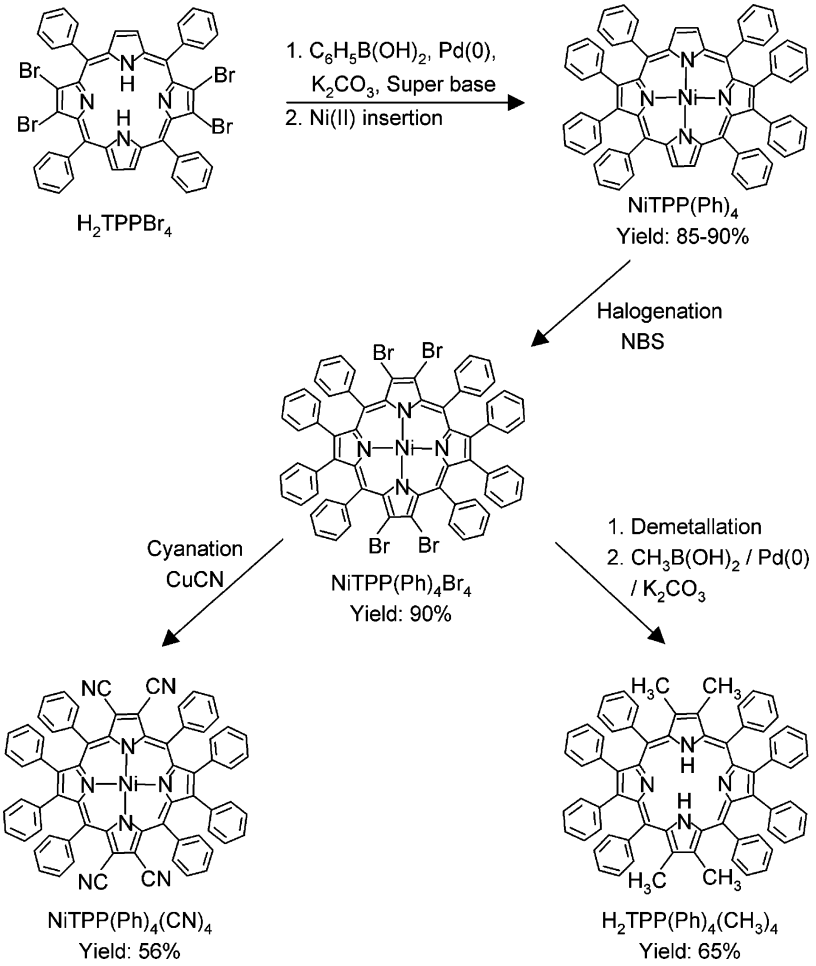

of these compounds are consistent with the reported values.[57] Earlier reports show that the Suzuki cross-coupling reaction with brominated porphyrins requires a longer reaction time (>4 days).[57] Halogenation (bromination or chlorination) of Ni(TPP(Ph)$_4$) with the *N*-halosuccinimide reagent produced the desired Ni(TPP(Ph)$_4$X$_4$) derivatives in 90% yield. The use of Ni(TPP(Ph)$_4$) was essential due to the considerable degradation of H$_2$(TPP(Ph)$_4$) or Zn(TPP(Ph)$_4$) derivatives in the presence of NXS (X = Br, Cl) in refluxing chloroform/1,1,2,2-tetrachloroethane. Further, the bromination of M(TPP(Ph)$_4$) [M = Cu(II), Ni(II)] was also carried out with liquid bromine and produced lower yields (40−50%) of the corresponding M(TPP(Ph)$_4$Br$_4$) derivatives.

The direct method was also examined as a way to synthesize M(TPP(Ph)$_4$(CH$_3$)$_4$ (M = 2H, Ni(II)) derivatives by the bromination of M(TPP(CH$_3$)$_4$) (M = 2H, Ni(II)) with NBS followed by the Suzuki cross-coupling reaction. This resulted in lower yields of the M(TPP(CH$_3$)$_4$Br$_4$) product. Hence, the synthesis of the H$_2$(TPP(Ph)$_4$(CH$_3$)$_4$) derivative was carried out using H$_2$(TPP(Ph)$_4$ as the precursor. Ni(TPPR$_4$(CN)$_4$) complexes were prepared in 40−55% yields by refluxing a Ni(TPPR$_4$Br$_4$) complex with an excess of CuCN in pyridine. The free-base mixed substituted porphyrin H$_2$(TPP(Ph)$_4$(CH$_3$)$_4$) derivative was prepared by the direct Suzuki cross-coupling reaction of H$_2$(TPP(Ph)$_4$Br$_4$) with methylboronic acid using Pd(0) catalyst. Other metal (Cu-

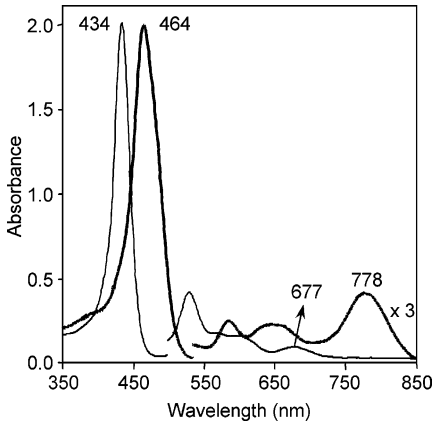

Figure 2. Electronic absorption spectra of H$_2$(TPP(Ph)$_4$) (thin line) and H$_2$(TPP(Ph)$_4$(CN)$_4$) (heavy line) in CH$_2$Cl$_2$ at 298 K. Q bands are magnified 3 times.

(II) and Zn(II)) complexes were prepared by demetalation of Ni(TPPR$_4$(CN)$_4$) with concentrated H$_2$SO$_4$. The desired metal insertion into the free-base porphyrins was performed using the reported procedures. Similar strategy was employed for the synthesis of MTPP(CH$_3$)$_4$X$_4$ compounds. All the synthesized compounds were characterized by electronic absorption, ^{1}H NMR, and mass spectral techniques.

Representative absorption spectra of H$_2$(TPP(Ph)$_4$(X)$_4$) (X = H, CN) derivatives are shown in Figure 2. Table 1 lists the electronic absorption spectral data for the M(TPP(Ph)$_4$X$_4$)

Table 1. Optical Absorption Spectral Data[a] of $MTPP(Ph)_4X_4$ Derivatives in CH_2Cl_2 at 298 K

porphyrin	B band (s), nm	Q band (s), nm
$H_2TPP(Ph)_4$	434 (5.45)	529 (4.29), 565 (sh), 599 (3.87), 677 (3.65)
$H_2TPP(Ph)_4(CH_3)_4$	368 (4.39), 457 (5.18)	555 (4.05), 607 (3.82), 704 (3.98)
$H_2TPP(Ph)_4Br_4$	377 (4.36), 470 (5.19)	574 (3.93), 630 (3.95), 734 (3.96)
$H_2TPP(Ph)_4Cl_4$	376 (4.39), 463 (5.23)	567 (3.90), 621 (3.97), 717 (4.03)
$H_2TPP(Ph)_4(CN)_4$	464 (5.14)	585 (3.97), 651 (3.99), 778 (4.16)
$NiTPP(Ph)_4$	431 (5.27)	548 (4.18), 585 (sh)
$NiTPP(Ph)_4(CH_3)_4$	439 (5.11)	558 (3.94), 607 (4.07)
$NiTPP(Ph)_4Br_4$	340 (4.22), 449 (5.15)	564 (4.00), 611 (3.84)
$NiTPP(Ph)_4Cl_4$	331 (4.39), 444 (5.33)	560 (4.19), 606 (4.00)
$NiTPP(Ph)_4(CN)_4$	344 (4.36), 457 (5.16)	545 (3.82), 592 (sh), 654 (4.48)
$CuTPP(Ph)_4$	428 (5.37)	554 (4.18), 593 (sh)
$CuTPP(Ph)_4(CH_3)_4$	345 (4.30), 458 (sh) 435 (5.19)	570 (4.12), 610 (4.02)
$CuTPP(Ph)_4Br_4$	357 (4.25), 466 (sh) 441 (5.07),	575 (4.05), 615 (sh)
$CuTPP(Ph)_4Cl_4$	354 (4.29), 459 (sh) 440 (5.15),	574 (4.11), 612 (sh)
$CuTPP(Ph)_4(CN)_4$	456 (5.10)	607 (sh), 662 (4.42)
$ZnTPP(Ph)_4$	431 (5.26)	559 (4.00), 601 (sh)
$ZnTPP(Ph)_4(CH_3)_4$	353 (4.35), 452 (5.15)	582 (4.02), 619 (3.83)
$ZnTPP(Ph)_4Br_4$	365 (4.37), 465 (5.23)	598 (4.04), 648 (4.00)
$ZnTPP(Ph)_4Cl_4$	364 (4.45), 456 (5.31)	587 (4.10), 634 (3.93)
$ZnTPP(Ph)_4(CN)_4$	466 (5.11)	626 (sh), 683 (4.33)

[a] Error in $\lambda_{max} = \pm 1.0$ nm; values in parentheses refer to $\log \epsilon$ (ϵ in $(dm^3/mol)/cm$); error in $\epsilon = \pm 7\%$.

compounds. $H_2(TPP(CH_3)_4X_4)$ (X = H, Br, CN) and $H_2(TPP(Ph)_4X_4)$ (X = H, Br, Cl, CH_3, CN) derivatives showed a Soret, B band, and three visible Q bands when compared to a B band and four Q bands of $H_2(TPP)$. $H_2(TPP(Ph)_4)$ exhibited red-shifts in the B band (20 nm) and in $Q_x(0,0)$ ($\sim$30 nm) bands relative to $H_2(TPP)$. This is possibly due to the β-pyrrole phenyl inductive interaction with the π-system rather than nonplanarity of the porphyrin macrocycle since it shows planar geometry.[57a] However, $H_2(TPP(CH_3)_4)$ shows marginal red-shift in the absorption bands relative to $H_2(TPP)$. The $M(TPPR_4)$ compounds (R = CH_3 or Ph; M = Ni(II), Cu(II), and Zn(II)) exhibited a B band and two Q bands with molar extinction coefficients similar to those of their corresponding M(TPP) compounds.[7,60]

The increase in size and number of β-pyrrole substituents induces greater steric crowding around the peripheral positions of the porphyrin; one would anticipate an increase in nonplanarity of the macrocycle that would lead to red-shift of the absorption bands.[61−63] The longest wavelength band, $Q_x(0,0)$, of the free-base mixed substituted porphyrins shows an interesting trend in red-shift and aligns in the following order: $H_2(TPP(Ph)_4(CH_3)_4) < H_2(TPP(Ph)_4Cl_4) < H_2(TPPR_4Br_4) < H_2(TPPR_4(CN)_4)$. Notably, of the mixed substituted porphyrins, $H_2(TPP(Ph)_4(CN)_4)$ shows a dramatic red-shift of 17−44 nm in the B band and 34−123 nm in the $Q_x(0,0)$ band relative to the corresponding bands of the β-tetrasubstituted $H_2(TPPX_4)$ (X = CH_3, Ph, Br, CN) derivatives.[42b,57,59] The red-shift in the sterically crowded porphyrins has been ascribed to the nonplanarity of the porphyrin ring in conjunction with the inductive or resonance interaction of the substituents that are in direct conjugation with the porphyrin π-system.

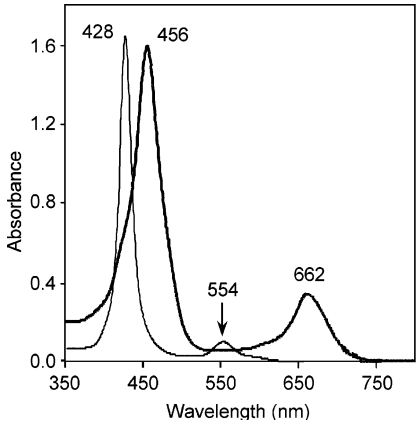

Figure 3. Optical absorption spectra of $Cu(TPP(Ph)_4)$ (thin line) and $Cu(TPP(Ph)_4(CN)_4$ (heavy line) in CH_2Cl_2 at 298 K.

Optical absorption spectra of a representative $Cu(TPP(Ph)_4X_4)$ (X = H, CN) are shown in Figure 3. The introduction of four more substituents on the other antipodal β-pyrrole positions of $M(TPP(Ph)_4)$ showed an interesting trend in their spectral features. Generally, metal complexes $M(TPPR_4X_4)$ exhibit a B band and two Q bands with the extent of red-shift of the B band being about 10−25 nm and 20−50 nm in Q(0,0) transitions relative to their corresponding $M(TPPX_4)$ (X = CH_3, CN, Br). Interestingly, $M(TPPR_4(CN)_4)$ complexes showed considerable gain in the intensity of the longest wavelength Q(0,0) band relative to the Q(1,0) band (Figure 3), and this is possibly due to stabilization of b_1 (a_{1_u}) relative to b_2 (a_{2_u}) and thereby further lifting of degeneracy of the highest occupied molecular orbitals (HOMOs).[62] As anticipated (Table 1), the bands are more blue-shifted with the increase in electronegativity of the metal ion.[64,65] Generally, $M(TPP(CH_3)_4X_4)$ derivatives show blue-shifted absorption spectral features relative to $M(TPP(Ph)_4X_4)$ derivatives. This is possibly due to the variable steric crowding that induces conformational differences between the macrocycles as well as the substituent effects. A pronounced red-shift in the absorption spectral features of the mixed substituted cyano and bromo porphyrins is due to both conjugative effect and nonplanar distortion of the porphyrin ring. Crystal structure studies on $Cu(TPP(Ph)_4$-

(60) Meot-Ner, M.; Adler, A. D. *J. Am. Chem. Soc*. **1975**, *97*, 5107.
(61) Barkigia, K. M.; Chantranupong, L.; Smith, K. M.; Fajer, J. *J. Am. Chem. Soc*. **1988**, *110*, 7566.
(62) Haddad, R. E.; Gazeau, S.; Pecaut, J.; Marchon, J.-C.; Medforth, C. J.; Shelnutt, J. A. *J. Am. Chem. Soc*. **2005**, *125*, 1253 and references therein.
(63) Parusel, A. B. J.; Tebikie, W.; Ghosh, A. *J. Am. Chem. Soc.* **2000**, *122*, 6371.
(64) Gouterman, M. *J. Chem. Phys.* **1959**, *30*, 1139.
(65) Ortiz, V.; Shelnutt, J. A. *J. Phys. Chem.* **1985**, *89*, 4733.

Table 2. Crystal Structure Data of Mixed Substituted Metalloporphyrins $Cu(TPP(Ph)_4(CH_3)_4)\cdot 2(CHCl_3)$ (**1**), $Zn(TPP(Ph)_4Br_4(CH_3OH))\cdot CH_3OH$ (**2**), and $Ni(TPP(Ph)_4(CN)_4(Py)_2)\cdot 2(Py)$ (**3**)

	1	**2**	**3**
empirical formula	$C_{74}H_{54}Cl_6N_4Cu$	$C_{70}H_{48}Br_4N_4O_2Zn$	$C_{92}H_{60}N_{12}Ni$
fw	1275.45	1380.15	1392.23
cryst syst	monoclinic	monoclinic	monoclinic
space group	*C*2/*c*	$P2_1/c$	*C*2/*c*
a (Å)	17.255(3)	13.848(6)	19.125(1)
b (Å)	20.397(2)	13.835(6)	18.531(1)
c (Å)	18.1490(15)	31.659(14)	21.8020
β (deg)	106.030(10)	97.49(4)	114.35(6)
vol (Å^3)	6139.2(13)	6014(5)	7038.8
Z	4	4	4
D_{calcd} (mg/m^3)	1.380	1.504	1.314
wavelength (Å)	1.541 80	0.710 69	1.541 80
T (K)	293	293	293
no. of total reflns	5585	10566	6399
no. of independent reflns	4949	4108	5206
R1[a]	0.0542	0.0754	0.0504
wR2[b]	0.1575	0.2144	0.1460

[a] $R1 = \sum||F_o| - |F_c||/\sum|F_o|$; $F_o > 4\sigma(F_o)$. [b] $wR2 = [\sum(F_o^2 - F_c^2)^2)/\sum w(F_o^2)^2]^{1/2}$.

$(CH_3)_4$) and $Zn(TPP(Ph)_4Br_4)$ show considerable nonplanar distortion of the porphyrin ring. The theoretical studies reported earlier predicted that the nonplanar porphyrins exhibit red-shift of the absorption bands.[62,63]

meso-Tetraphenylporphyrin, $H_2(TPP)$, exhibits characteristic chemical shifts arising from the β-pyrrole and *meso*-phenyl proton resonances.[66] The ^1H NMR spectra of free-base mixed substituted porphyrins ($H_2(TPP(Ph)_4X_4)$ (X = CH_3, Cl, Br, CN) exhibit resonances arising from *meso*- and β-pyrrole phenyls, β-methyl and imino hydrogens. The chemical shifts of the *meso*-phenyl protons of $H_2(TPP(Ph)_4X_4)$ (X = CH_3, Cl, Br, H) are comparable to those observed for the corresponding $H_2(TPP(Ph)_4)$ derivative. The core imino-protons of $H_2(TPP(Ph)_4X_4)$ (X = Cl, Br, CH_3) (−1.65 ppm) are downfield-shifted relative to $H_2(TPP(Ph)_4)$ (−2.13 ppm).[57c] Further, the $H_2(TPP(Ph)_4(CN)_4)$ derivative shows imino-proton resonance at −2.20 ppm. The downfield shift of the resonances is possibly due to the nonplanar conformation and/or substituent effects. Similar trends in chemical shifts of imino-protons were observed for $H_2(TPP(CH_3)_4X_4)$ derivatives. Nonplanarity of the macrocycle causes the imino-protons to resonate at downfield relative to that in planar porphyrins.[67] The ^1H NMR spectra of $M(TPPR_4X_4)$ (M = Zn(II) and Ni(II)) complexes are devoid of imino-protons, and their other proton resonances are marginally upfielded (0.1−0.3 ppm) relative to those of the $H_2(TPP(Ph)_4X_4)$ derivative. The integrated intensity of the proton resonances of these mixed substituted porphyrins ($M(TPPR_4X_4)$) is consistent with the proposed structures.

Crystal Structure Discussion. Crystallographic data of the $Cu(TPP(Ph)_4(CH_3)_4)$ and $Zn(TPP(Ph)_4Br_4)$ complexes are listed in Table 2. ORTEP views (top and side) of the $Cu(TPP(Ph)_4(CH_3)_4$ and $Zn(TPP(Ph)_4Br_4)$ complexes are shown in Figures 4 and 5, respectively. The selected average bond lengths and bond angles of $Cu(TPP(Ph)_4(CH_3)_4)\cdot 2(CHCl_3)$ and $Zn(TPP(Ph)_4Br_4)(CH_3OH)\cdot CH_3OH$ structures are compared with the reported $Zn(TPP(Ph)_8)$ structure to examine the role of mixed substitution on the stereochemical features (Table 3). The Cu−N and Zn−N bond distances observed in these complexes are similar to those reported for their corresponding M−N bond distances.[68] Nonequivalent distances in the M−N and M−N′ of the M−$(N)_4$ core in these mixed substituted porphyrins are possibly due to electronic and steric strain induced by the peripheral substituents.[50,69] The extent of steric crowding arising from the methyl (van der Waals radius (VDW), 2.0 Å) group is anticipated to be higher than that of bromo group (VDW, 1.95 Å).[70] The more

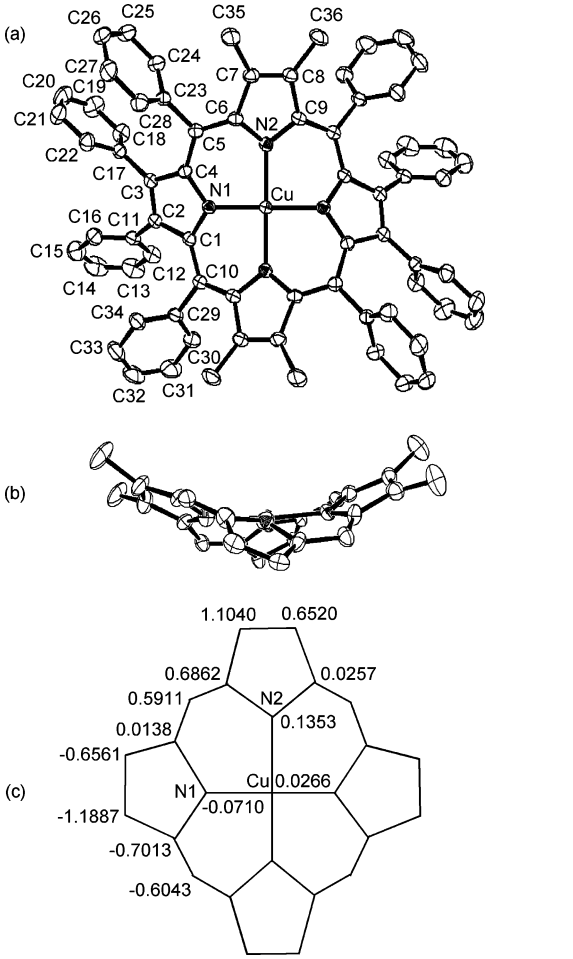

Figure 4. ORTEP diagrams showing (a) top and (b) side views of $Cu(TPP(Ph)_4(CH_3)_4)\cdot 2CHCl_3$. The solvates and the hydrogens are not shown for clarity, and in the side view, the phenyl groups are not shown for simplicity. Displacement of porphyrin-core atoms in Å from the mean plane (esd's 0.003 Å) is shown in part c.

(66) Scheer, H.; Katz, J. J. In *Porphyrins and Metalloporphyrins;* Smith, K. M., Ed.; Elsevier: Amsterdam, The Netherlands, 1975; p 399.
(67) Smirnov, V. V.; Woller, E. K.; DiMagno, S. G. *Inorg. Chem.* **1998**, *37*, 4971.
(68) Scheidt, W. R.; Lee, Y. J. *Struct. Bonding (Berlin)* **1987**, *64*, 1.
(69) Scheidt, W. R. In *The Porphyrin Handbook;* Kadish, K. M., Smith, K. M., Guilard, R., Eds.; Academic Press: New York, 2000; Vol. 3, p 49.
(70) Cotton F. A.; Wilkinson, G. *Advanced Inorganic Chemistry*, 3rd ed.; Interscience Publishers: New York, 1972.
(71) Barkigia, K. M.; Nurco, D. J.; Renner, M. W.; Melamed, D.; Smith, K. M.; Fajer, J. *J. Phys. Chem. B* **1998**, *102*, 322.

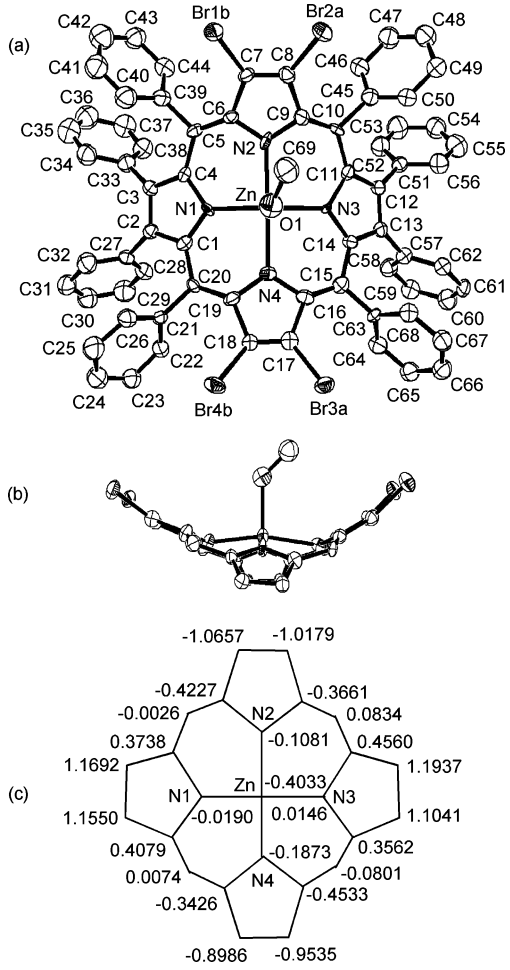

Figure 5. ORTEP diagrams showing (a) top and (b) side views of the $Zn(TPP(Ph)_4Br_4(CH_3OH))\cdot CH_3OH$ complex. The lattice solvates and hydrogens are omitted for clarity. Displacement of porphyrin-core atoms from the mean plane in Å (esd's 0.008 Å) is shown in part c.

donor effect of the methyl group enhances the electron density on the pyrrole nitrogens than phenyl groups, and hence in the $Cu(TPP(Ph)_4(CH_3)_4)$ complex, the Cu−N′ pair shows a shorter distance than the Cu−N distance (Table 3). Similarly, the $Zn(TPP(Ph)_4Br_4)(CH_3OH)\cdot(CH_3OH)$ complex shows longer Zn−N′ bond lengths for pyrroles with bromo groups and shorter M−N bond distances for pyrroles bearing phenyl rings. Earlier reports on $Zn(TPPBr_4(CH_3OH))\cdot DMF$ and $Ni(TPPBr_4(CN)_4)$ structures showed longer M−N (for the pyrroles with more electron withdrawing substituents) distances due to decreased electron density on the imino-nitrogens.[42a,50]

The nonplanarity of the porphyrin core is induced by the steric repulsion among the peripheral substituents, which enforces the relief of the strain through bond lengths and angles. For the mixed substituted porphyrin structures, one would anticipate difference in crowding along the antipodal positions because of the variable shape and size of the β-pyrrole substituents. Nonplanar conformation arises by the tilting of the pyrroles to prevent repulsive interactions among the substituents, and this results in an increase of the $C_\beta-C_\alpha-C_m$ angles with the concomitant decrease in the $N-C_\alpha-C_m$ and $M-N-C_\alpha$ angles. The $Cu(TPP(Ph)_4(CH_3)_4)$ and $Zn(TPP(Ph)_4Br_4)$ exhibited about a 2−7° change in these

Table 3. Selected Bond Lengths and Geometric Parameters of Substituted Metalloporphyrins

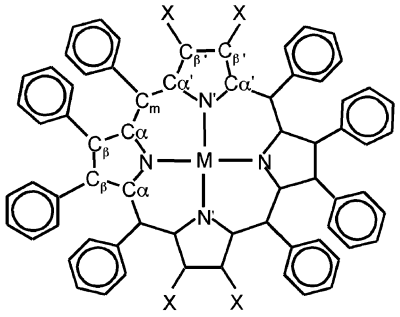

M = Cu(II), X = CH_3, $Cu(TPP(Ph)_4(CH_3)_4)$
M = Zn(II), X = Br, $Zn(TPP(Ph)_4Br_4)$
M = Zn(II), X = Ph, $Zn(TPP(Ph)_8)$

	$Cu(TPP(Ph)_4(CH_3))_4$	$Zn(TPP(Ph)_4Br_4))$	$Zn(TPP(Ph)_8)^a$
	Bond Length (Å)		
M−N	1.962(2)	2.001(7)	2.037(4)
M−N′	1.946(2)	2.102(7)	
M−O		2.044(8)	
$N-C_\alpha$	1.376(3)	1.401(10)	1.376(3)
$N'-C_\alpha$	1.373(3)	1.407(10)	
$C_\alpha-C_\beta$	1.454(4)	1.426(11)	1.456(4)
$C_{\alpha'}-C_{\beta'}$	1.452(4)	1.505(12)	
$C_\beta-C_\beta$	1.371(4)	1.375(11)	1.371(6)
$C_{\beta'}-C_{\beta'}$	1.363(4)	1.294(11)	
$C_\alpha-C_m$	1.410(4)	1.326(12)	1.412(11)
$C_{\alpha'}-C_m$	1.404(4)	1.449(11)	
$\Delta C_\beta{}^b$ (Å)	0.90	1.07	0.96
	Bond Angle (deg)		
$M-N-C_\alpha$	124.4(1)	126.9(5)	124.4(2)
$M-N'-C_\alpha$	125.1(2)	119.6(6)	
$N-C_\alpha-C_m$	122.2(2)	120.8(8)	123.2(3)
$N'-C_{\alpha'}-C_m$	122.9(2)	123.8(8)	
$N-C_\alpha-C_\beta$	109.1(2)	111.7(8)	109.2(3)
$N'-C_{\alpha'}-C_{\beta'}$	108.9(2)	102.8(7)	
$C_\beta-C_\alpha-C_m$	128.1(2)	127.4(9)	127.5(3)
$C_{\beta'}-C_{\alpha'}-C_m$	127.7(2)	132.7(9)	
$C_\alpha-C_m-C_{\alpha'}$	122.5(2)	124.6(8)	124.5(3)
$C_{\alpha'}-C_m-C_\alpha$	122.1(2)	124.6(8)	
$C_\alpha-C_\beta-C_\beta$	106.9(2)	106.7(8)	107.0(2)
$C_{\alpha'}-C_{\beta'}-C_{\beta'}$	107.1(2)	110.5(8)	

[a] Data from ref 71. [b] Average deviation of β-pyrrole carbon from the 24-atom mean plane.

angles, and this change is comparable to that of the saddle shaped $Zn(TPP(Ph)_8)$ structure (Table 3). The methyl group of the axially coordinated methanol in $Zn(TPP(Ph)_4Br_4)$ shows some positional disorder. It is noteworthy that the Zn(II) ion is about 0.4033 Å above the mean plane, higher than that reported for the $Zn(TPPBr_4(CH_3OH))$ complex (0.28 Å),[42] and it is 0.07 Å in the case of the four-coordinated $Zn(TPP(Ph)_8)$ complex.[71] Another reported five-coordinated $Zn(TPP(Ph)_8(CH_3CN))$ structure shows a 0.233 Å displacement of Zn(II) ion from the mean plane with moderate saddling of the core ($\Delta C_\beta = \pm 0.43$ Å).[72] Steric and electronic factors are responsible for the extent of displacement of the zinc(II) ion from the mean plane of the 24-atom core. The observed distortions in these porphyrins are larger than those reported for partially substituted $Zn(TPPBr_4)$ complexes.[42,54] Moreover, the N1−M−N3 and N2−M−N4 angles are deviated from 180° indicating the nonplanar

(72) Harada, R.; Kojima, T. *Acta Crystallogr.* **2002**, *E60*, 1097.

conformation of the M−$(N)_4$ core. Each pyrrole ring is alternately displaced up and down from the mean plane formed by the 24-atom core. The magnitude of displacements for the β-pyrrole carbons bearing mixed substituents from the mean plane is unequal along the antipodal directions. The phenyl groups are tilted toward the macrocycle plane to minimize the repulsive interaction between the substituents. The phenyl and bromo groups at the β-pyrrole positions are titled up and down from the porphyrin mean plane to minimize steric crowding between the substituents. The average dihedral angles formed by the *meso*-phenyl (53−56°) are lower in contrast to that formed by the β-pyrrole phenyl groups (65−70°) with the porphyrin plane for Zn(TPP$(Ph)_4Br_4$) and Cu(TPP$(Ph)_4(CH_3)_4$) structures. The average bond lengths of the C_m−*meso*-C_{ph} and C_β−C_β(Ph) in Zn(TPP$(Ph)_4Br_4$) and Cu(TPP$(Ph)_4(CH_3)_4$) are found to be 1.48−1.50 Å, indicating no significant conjugation of the phenyl rings with the porphyrin macrocycle although the phenyl groups are tilted toward the porphyrin plane. The extent of observed macrocyclic distortions is similar to that of fully β-octaalkylated-MTPPs,[73] β-octaphenylated-MTPPs[71,74] and Zn(TPPBr_8(butyronitrile)$_2$)[75] structures. In the case of Zn(TPP$(Ph)_4Br_4(CH_3OH)$)·CH_3OH, the lattice solvate is weakly hydrogen bonded to the coordinated methanol with the shortest O···O distance of 2.908 Å.[76]

The extent of mean plane deviation of the atoms in Cu(TPP$(Ph)_4(CH_3)_4$) and Zn(TPP$(Ph)_4Br_4$) is shown in Figures 4c and 5c, respectively. The 24-atom core of the Cu(TPP$(Ph)_4(CH_3)_4$) complex (Figure 4c) shows a combination of saddle with severe ruffled conformation, whereas ZnTPP$(Ph)_4Br_4$ has more saddling of the core with very gentle ruffled conformation (Figure 5c). As anticipated for saddle conformations, the dihedral angles for the *meso*-phenyl rings are smaller than those observed for more planar macrocycles.[68] The size and number of β-pyrrole substituents of MTPP induce varying degrees of nonplanarity to the porphyrin macrocycle. It is known in the literature that the partially brominated porphyrins, Zn(TPP$Br_4(CH_3OH)$),[42] ZnTPPBr_4(tetrahydrofuran),[54] and tetrabromo-tetramesitylporphyrins,[48] exhibit moderate distortion of the porphyrin core. The β-octahalogenotetraarylporphyrins, octabromotetraphenylporphinato zinc(II) dibutyronitrile,[75] octabromotetrakis(pentafluorophenyl)porphinato zinc(II) hydrate,[77] octabromotetrakis(2,6-dibromo-3,5-dimethoxyphenyl)porphinato copper(II) methanol,[29] octabromotetraphenylporphinato nickel,[78] copper(II) and nickel(II) complexes of octabromotetrakispentafluorophenylporphyrins,[79] octachloro-*meso*-tetrakis(pentafluorophenyl)porphinato zinc(II),[80] octafluorotetraphenylporphinato zinc(II),[30,31] and octafluorotetrakis(pentafluorophenyl)porphinato zinc(II),[81] showed nonplanar distortion of the porphyrin core. The nonplanar distortion of the mixed substituted Zn(II) and Cu(II) porphyrins has been largely due to the steric crowding of the peripheral groups to minimize the repulsive interactions among the substituents. The closest distance between the porphyrin units is more than 3.40 Å indicating the nonplanar conformation in these systems is influenced by the repulsive interactions among the peripheral groups. This also suggests the $\pi-\pi$ interactions between the phenyl rings of the porphyrin macrocycles in the lattice are negligible.

The crystal structure of the six-coordinated complex Ni(TPP$(Ph)_4(CN)_4(Py)_2$)·2Py was examined to determine the role of cyano and phenyl groups at the β-pyrrole positions on the stereochemistry of the coordinated nickel(II) porphyrin complex. The crystallographic data of the complex are shown in Table 2. Its molecular structure is shown along with the numbering scheme in Figure 6a. Figure 6b,c shows the side on view and the perpendicular displacement of all the skeletal atoms from the 24-atom core mean plane, respectively. A comparison of Ni(TPP$(Ph)_4(CN)_4)(Py)_2$) is made with the reported Ni(TPP$Br_4(CN)_4)(Py)_2$) structure (Table 4) to examine the role of mixed β-pyrrole (phenyl and cyano vs bromo and cyano) groups on the structural changes. The geometry around the Ni(II) center, axial Ni−$N_{pyridine}$ and equatorial Ni−N bond lengths of the structure (Table 4), seems to suggest that the Ni(II) is in the typical $S = 1$ spin system rather than in the four-coordinate Ni(II) porphyrins with shorter Ni−N distances of Ni(II) ($S = 0$) systems.[82] As reported previously, the four-coordinate low-spin Ni(II) porphyrins[82] tend to show shorter Ni−N bond lengths than the six-coordinate high-spin[50] Ni(II) porphyrin complexes. The six-coordinate structure of the Ni(TPP$(Ph)_4(CN)_4(py)_2$)·2Py complex is possibly due to the electron deficiency of the Ni(II) center induced by the electron deficiency of the porphyrin macrocycle. Interestingly, the Ni−N (for the pyrrole with CN groups) distance seems to be shorter than the Ni−N′ distance (for the pyrrole with phenyl groups) (Table 4). A similar trend in Ni−N bond distances was reported for the Ni(TPP$Br_4(CN)_4(Py)_2$)·2.5$(C_2H_4Cl_2)$ structure.[50] The expansion of the porphyrin core in the Ni(TPP$(Ph)_4(CN)_4(Py)_2$)·2Py complex is reflected from the bond lengths (N−C_α and C_α−C_m) and angles (C_α−N−C_α, N−C_α−C_m, and N−C_α−C_β), and it is similar to that found in the

(73) Barkigia, K. M.; Berber, M. D.; Fajer, J.; Medforth, C. J.; Renner, M. W.; Smith, K. M. *J. Am. Chem. Soc.* **1990**, *112*, 8851.
(74) Nurco, D. J.; Medforth, C. J.; Forsyth, T. P.; Olmstead, M. M.; Smith, K. M. *J. Am. Chem. Soc.* **1996**, *118*, 10918.
(75) Bhyrappa, P.; Krishnan, V.; Nethaji, M. *J. Chem. Soc., Dalton Trans.* **1993**, 1901.
(76) Bhyrappa, P.; Wilson, S. R.; Suslick, K. S. *J. Am. Chem. Soc.* **1997**, *119*, 8492.
(77) Marsh, R. E.; Schaeffer, W. P.; Hodge, J. A.; Hughes, M. E.; Gray, H. B.; Lyons, J. E.; Ellis, P., Jr. *Acta Crystallogr.* **1993**, *C49*, 1339.
(78) Mandon, D.; Ochsenbein, P.; Fischer, J.; Weiss, R.; Jayaraj, K.; Austin, R. N.; Gold, A.; White, P. S.; Brigaud, O.; Battioni, P.; Mansuy, D. *Inorg. Chem.* **1992**, *31*, 2044.
(79) Henling, L. M.; Schaefer, W. P.; Hodge, J. A.; Hughes, M. E.; Gray, H. B. *Acta Crystallogr.* **1993**, *C49*, 1743.
(80) Birnbaum, E. R.; Hodge, J. A.; Grinstaff, M. W.; Schaefer, W. P.; Henling, L.; Labinger, J. A.; Bercaw, J. E.; Gray, H. B. *Inorg. Chem.* **1995**, *34*, 3625.
(81) Smirnov, V. V.; Woller, E. K.; Tatman, D.; DiMagno, S. G. *Inorg. Chem.* **2001**, *40*, 2614.
(82) (a) Scheidt, W. R. In *The Porphyrins;* Dolphin, D., Ed.; Academic Press: New York, 1978; Vol. 3, p 463. (b) Barkigia, C. M.; Renner, M. W.; Furenlid, L. R.; Medforth, C. J.; Smith, K. M.; Fajer, J. *J. Am. Chem. Soc.* **1993**, *115*, 3627. (c) Hobbs, J. D.; Majumder, S. A.; Luo, L.; Sickelsmith, G. A.; Auirke, J. M. E.; Medforth, C. J.; Smith, K. M.; Shelnutt, J. A. *J. Am. Chem. Soc.* **1994**, *116*, 3261. (d)Veyarath, M.; Ramassuel, R.; Marchon, J. C.; Turovska-Tyrk, I.; Scheidt, W. R. *New J. Chem.* **1995**, *19*, 1199.

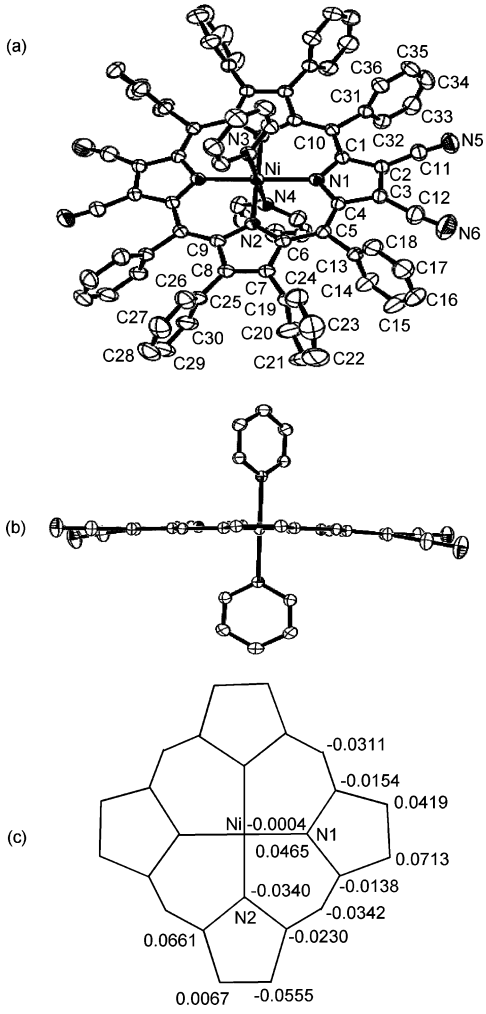

Figure 6. ORTEP diagrams showing (a) top and (b) side views of the $Ni(TPP(Ph)_4(CN)_4(Py)_2)\cdot 2Py$ complex. The lattice solvates and hydrogens are omitted for clarity. In the side view, the phenyl groups are not shown for simplicity. Displacements of the porphyrin-core atoms from the mean plane in Å (esd's 0.0017) are shown in part c.

six-coordinated $Ni(TPPBr_4(CN)_4(Py)_2)\cdot 2.5(C_2H_4Cl_2)$ complex (Table 4). Another interesting feature of the complex is that the $Ni-N_{pyridine}$ bond distance (2.216(3) Å) in $Ni(TPP)(Ph)_4(CN)_4(Py)_2)\cdot 2Py$ is longer than that reported for the mixed substituted $Ni(TPPBr_4(CN)_4(Py)_2)\cdot 2.5(C_2H_4Cl_2)$ complex (2.153(3) Å) and shorter than that found in the $Ni(TPP(CN)_4(Py)_2)$ complex (2.242(2) Å).[83] The two axially ligated pyridine rings are almost planar, and their planes are perpendicular to each other. Furthermore, the axial $(Ni-N_{pyridine})_{av}$ distance is longer than the equatorial $(Ni-N)_{av}$ distance, but it is similar to that reported for $Ni(TPPBr_4(CN)_4(Py)_2)\cdot 2.5C_2H_4Cl_2$ structure (Table 4). In the case of the $Ni(TPP(Ph)_4(CN)_4(Py)_2)\cdot 2Py$ structure, the two axially coordinated pyridines are in an almost mutually perpendicular orientation, and the axial pyridine mean planes make dihedral angles[68] close to 45° (42.2 and 49°) with the closest equatorial Ni−N axis. Similar features were reported previously for $Ni(TPPBr_4(CN)_4(Py)_2\cdot 2.5(C_2H_4Cl_2)$[50] and other iron porphyrins.[84] The staggered orientation of the axially ligated pyridines is probably due to favorable back-donation from the nickel $d\pi(d_{xz}, d_{yz})$ to the π^* orbitals of the pyridines and also reduces the nonbonding interactions between the axial pyridines with the porphyrin ring.

Surprisingly, the mean plane displacement of core atoms in the $Ni(TPP(Ph)_4(CN)_4(Py)_2)\cdot 2Py$ complex (Figure 6c) shows very minimal wavelike conformation in contrast to ruffling combined with the moderate saddling of the porphyrin macrocycle reported for the $Ni((TPP)Br_4(CN)_4(Py)_2\cdot 2.5(C_2H_4Cl_2)$ complex. This is reflected from the mean plane displacement of β-pyrrole carbons (Table 4) and *meso*-

Table 4. Selected Bond Lengths and Geometric Parameters of $Ni(TPP(Ph)_4(CN)_4(Py)_2)\cdot 2(Py)$ and $Ni(TPPBr_4(CN)_4(Py)_2)\cdot 2.5(C_2H_4Cl_2)$ Structures

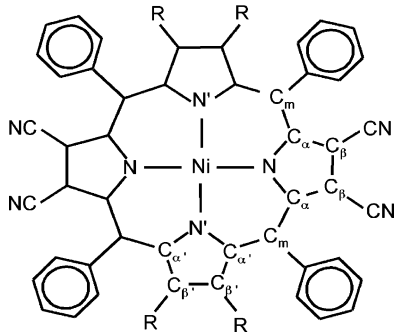

R = Ph, $Ni(TPP(Ph)_4(CN_4))$

R = Br, $Ni(TPPBr_4(CN)_4)$

	$Ni(TPP(Ph)_4(CN)_4(Py)_2)$	$Ni(TPPBr_4(CN)_4(Py)_2)$[a]
	Bond Length (Å)	
Ni−N	2.051(2)	2.040(2)
Ni−N′	2.089(2)	2.073(2)
$Ni-N_{pyridine}$	2.216(3)	2.153(3)
$N-C_\alpha$	1.369(3)	1.367(3)
$N'-C_{\alpha'}$	1.375(3)	1.375(3)
$C_\alpha-C_\beta$	1.438(1)	1.441(3)
$C_{\alpha'}-C_{\beta'}$	1.462(3)	1.463(3)
$C_\beta-C_\beta$	1.371(3)	1.371(4)
$C_{\beta'}-C_{\beta'}$	1.356(3)	1.341(4)
$C_\alpha-C_m$	1.409(3)	1.405(8)
$C_{\alpha'}-C_m$	1.402(3)	
ΔC_β[b] (Å)	0.0438	0.625
	Bond Angles (deg)	
$Ni-N-C_\alpha$	125.7(1)	124.9(3)
$Ni-N'-C_{\alpha'}$	126.3(2)	125.1(3)
$N-C_\alpha-C_m$	127.0(2)	126.0(2)
$N'-C_{\alpha'}-C_m$	125.0(2)	124.6(2)
$N-C_\alpha-C_\beta$	108.6(2)	108.6(2)
$N'-C_{\alpha'}-C_{\beta'}$	109.3(2)	108.1(2)
$C_\beta-C_\alpha-C_m$	124.4(2)	125.3(4)
$C_{\beta'}-C_{\alpha'}-C_m$	125.7(2)	127.2(4)
$C_\alpha-C_m-C_{\alpha'}$	125.4(2)	124.6(2)
$C_\alpha-C_\beta-C_\beta$	107.2(2)	107.1(2)
$C_{\alpha'}-C_{\beta'}-C_{\beta'}$	107.1(2)	107.6(2)
$C_\alpha-N-C_\alpha$	108.4(2)	108.4(2)
$C_{\alpha'}-N'-C_{\alpha'}$	107.3(2)	108.2(2)

[a] Data from ref 50. [b] Average deviation of β-pyrrole carbon atom from the 24-atom mean plane.

(83) Duval, H.; Bulach, V.; Fischer, J.; Weiss, R. *Acta Crystallogr*. **1997**, *C53*, 1027.

(84) (a) Munro, O. Q.; Marques, H. M.; Debrunner, P. G.; Mohanrao, K.; Scheidt, W. R. *J. Am. Chem. Soc.* **1995**, *117*, 935. (b) Grinstaff, M. W.; Hill, M. G.; Birnbaum, E. R.; Schaefer, W. P.; Labinger, J. A.; Gray, H. B. *Inorg. Chem.* **1995**, *34*, 4896. (c) Safo, M. K.; Walker, F. A.; Raitsimring, A. M.; Walters, W. P.; Dolata, D. P.; Debrunner, P. G.; Scheidt, W. R. *J. Am. Chem. Soc.* **1994**, *116*, 7760. (d) Safo, M. K.; Gupta, G. P.; Watson, C. T.; Simonis, U.; Walker, F. A.; Scheidt, W. R. *J. Am. Chem. Soc.* **1992**, *114*, 7066.

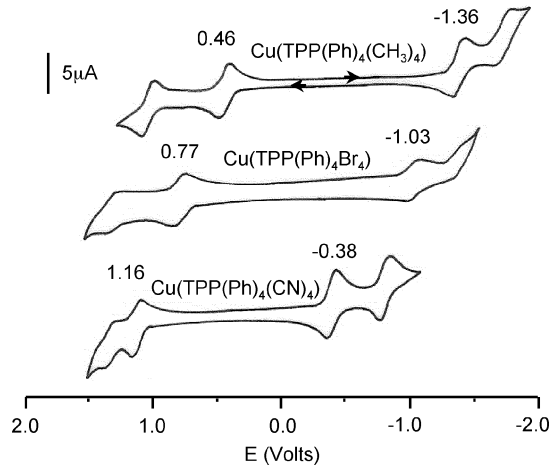

Figure 7. Cyclic voltammograms of $CuTPP(Ph)_4X_4$ (X = CH_3, Br, CN) complexes in CH_2Cl_2 containing 0.1 M $TBAPF_6$ with a scan rate of 0.1 V/s at 298 K.

carbons (Figure 6c). Further, the phenyl groups are oriented perpendicular to the mean plane of the porphyrin ring with a dihedral angle of 81.2° and 80.3° for the *meso*-phenyl and β-pyrrole phenyl groups, respectively. The nearly planar conformation of the porphyrin macrocycle in $Ni(TPP(Ph)_4(CN)_4(Py)_2)\cdot 2Py$ is probably due to the decreased steric crowding at the antipodal positions compared to that of the $Ni(TPPBr_4(CN)_4)\cdot 2.5(C_2H_4Cl_2)$ complex rather than any intermolecular interactions since the closest intermolecular contact in $NiTPP(Ph)_4(CN)_4(Py)_2\cdot 2Py$ is greater than 3.394 Å.

Electrochemistry. To probe the influence of mixed β-pyrrole substitution on the π-electronic properties of the $MTPPR_4X_4$ compounds (M = 2H, Ni(II), Cu(II), and Zn(II)), the electrochemical redox behavior of these porphyrins was examined by cyclic voltammetric studies. Figure 7 shows the cyclic voltammograms of $CuTPP(Ph)_4X_4$ bearing varying β-pyrrole substituents. The effect of core metal ion on the redox potentials of the representative porphyrins $MTPP(Ph)_4Cl_4$ (M = Ni(II), Cu(II) and Zn(II)) is shown in Figure 8. Table 5 lists the electrochemical data for the $MTPP(Ph)_4X_4$ complexes. Under similar conditions, the corresponding MTPP compounds were also examined and the data is listed in Table 5. The data analysis of free-base and metal complexes of the mixed substituted porphyrins $MTPPR_4X_4$ (X = H, CH_3, Br, Cl, CN) series indicates the following observations: (1) The mixed substituted porphyrins show two successive one-electron electrochemical oxidations and reductions. (2) Notably, the first ring oxidation potentials span a range from 0.38 to 1.36 V while reduction potentials vary from −0.28 to −1.5 V. (3) For the Hammett equation $E_{1/2} = 4\sigma\rho$, the plot of the first ring oxidation and reduction versus the Hammett parameter[85] (σ_p) of the substituents (X) in $MTPPR_4X_4$ was examined to delineate the role of X on the potentials of $MTPPR_4$, and they show more linear trend in reduction than in oxidation (Figure 9 and Table 6). (4) The reaction constant (ρ) for the oxidation and reduction is

(85) The Hammett parameter (σ_p) of the substituents (X) was taken from the following: Hansch, C.; Leo, A.; Taft, R. W. *Chem. Rev.* **1991**, *91*, 165.

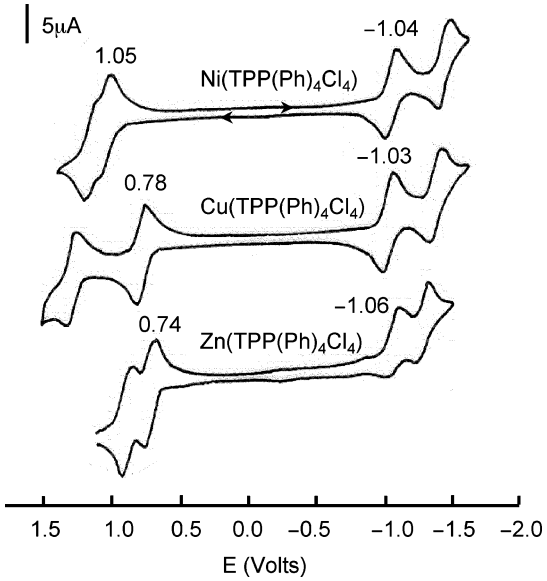

Figure 8. Cyclic voltammograms of $MTPP(Ph)_4Cl_4$ complexes in CH_2Cl_2 containing 0.1 M $TBAPF_6$ with a scan rate of 0.10 V/s at 298 K.

Table 5. Half-Wave Electrochemical Redox Data[a] (vs Ag/AgCl) of $M(TPP(Ph)_4X_4)$ Derivatives in CH_2Cl_2 Containing 0.1 M $TBAPF_6$ at 298 K

	oxidation (V)			reduction (V)	
porphyrin	I	II	$\Delta E_{1/2}$[d] (V)	I	II
$H_2(TPP)$	1.00	1.34	2.23	−1.23	−1.54
$H_2(TPP(Ph)_4)$	0.83	0.95	2.02	−1.19	
$H_2(TPP(Ph)_4(CH_3)_4)$	0.59	0.84	1.79	−1.20	
$H_2(TPP(Ph)_4Br_4)$	0.82	0.93	1.70	−0.88	−1.25
$H_2(TPP(Ph)_4Cl_4)$	0.86	0.98	1.77	−0.91	−1.03
$H_2(TPP(Ph)_4(CN)_4)$	1.13	1.38	1.41	−0.28	−0.56
Ni(TPP)	1.02	1.32	2.30	−1.28	−1.72
$Ni(TPP(Ph)_4)$	0.91	1.19	2.23	−1.32	−1.71
$Ni(TPP(Ph)_4(CH_3)_4)$	0.72	1.03	2.12	−1.40	−1.74
$Ni(TPP(Ph)_4Br_4)$	1.02	1.17	2.05	−1.03	−1.32
$Ni(TPP(Ph)_4Cl_4)$	1.05	1.17	2.09	−1.04	−1.42
$Ni(TPP(Ph)_4(CN)_4)$	1.36[b]		1.78	−0.42	−0.86
Cu(TPP)	0.97	1.35	2.27	−1.30	−1.70
$Cu(TPP(Ph)_4)$	0.75	1.26	2.08	−1.33	−1.57
$Cu(TPP(Ph)_4(CH_3)_4)$	0.46	1.04	1.82	−1.36	−1.70
$Cu(TPP(Ph)_4Br_4)$	0.77	1.29	1.80	−1.03	−1.32
$Cu(TPP(Ph)_4Cl_4)$	0.78	1.29	1.81	−1.03	−1.38
$Cu(TPP(Ph)_4(CN)_4)$	1.16	1.38	1.54	−0.38	−0.80
Zn(TPP)	0.84	1.15	2.20	−1.36	−1.77
$Zn(TPP(Ph)_4)$	0.74	0.88	2.13	−1.39	−1.79
$Zn(TPP(Ph)_4(CH_3)_4)$	0.38	0.66	1.88	−1.50	−1.67[c]
$Zn(TPP(Ph)_4Br_4)$	0.72	0.90	1.78	−1.06	−1.27
$Zn(TPP(Ph)_4Cl_4)$	0.74	0.88	1.80	−1.06	−1.27
$Zn(TPP(Ph)_4(CN)_4)$	1.02	1.35	1.48	−0.46	−0.82

[a] Error in redox potentials = ±10 mV; scan rate = 0.1 V/s. [b] Two electron oxidation. [c] Irreversible. [d] ^{I}oxidation − ^{I}reduction.

in the range 0.15−0.22 and 0.29−0.38 V, respectively. (5) The first ring redox potentials are cathodic (0.03−0.10 mV) for the $MTPP(CH_3)_4X_4$ series relative to the $MTPP(Ph)_4X_4$ series. (6) The difference in the first ring redox potential (HOMO−LUMO gap) is narrower (Table 5) with the increase in the Hammett parameter of the substituents.

Interestingly, the first oxidation potentials of $MTPPR_4X_4$ are more cathodically shifted (150−500 mV) while reduction potentials are marginally cathodic (~50 mV) relative to their corresponding $MTPPX_4$ (X = CN, Br) derivatives.[38−40,42] The reactivity constant, ρ, for the $MTPP(Ph)_4X_4$ is comparable

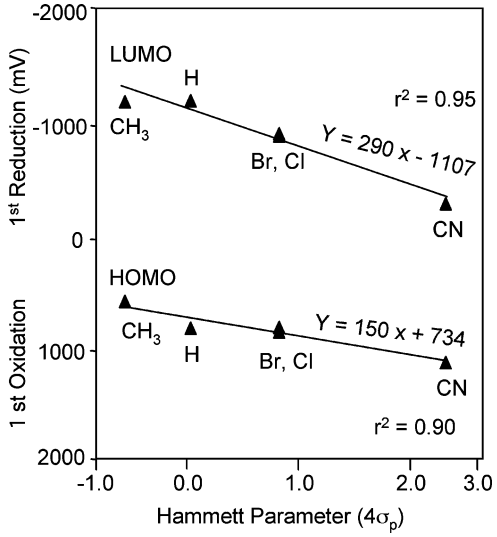

Figure 9. Plot of first ring redox potentials versus the Hammett parameter (σ_p) of the substituents (X) for $H_2TPP(Ph)_4(X)_4$ derivatives.

Table 6. Summary of Hammett Plots with Reaction Constants (ρ) and Correlation Coefficients (r^2) of First Ring Redox Potentials for Various Mixed Substituted Porphyrins[a]

	first oxidation		first reduction	
porphyrin	ρ (V)	r^2	ρ (V)	r^2
$H_2(TPP(Ph)_4X_4)$	0.150	0.906	0.290	0.950
$Ni(TPP(Ph)_4X_4)$	0.190	0.987	0.300	0.975
$Cu(TPP(Ph)_4X_4)$	0.190	0.926	0.310	0.956
$Zn(TPP(Ph)_4X_4)$	0.170	0.842	0.320	0.988
$H_2(TPP(CH_3)_4X_4)$	0.150	0.797	0.330	0.993
$Ni(TPP(CH_3)_4X_4)$	0.220	0.903	0.350	0.998
$Cu(TPP(CH_3)_4X_4)$	0.220	0.863	0.340	0.999
$Zn(TPP(CH_3)_4X_4)$	0.170	0.717	0.375	0.967

[a] $MTPPR_4X_4$: R= Ph, X = CH_3, H, Br, Cl, CN; R = CH_3, X = Ph, H, Br, CN.

to that of the partially β-pyrrole substituted-TPP series,[39] and it is considerably higher than that reported for the β-octahalo-MT(4-X-phenyl)P series[86] or MT(4-X-phenyl)P series.[87] The fairly broader range of ρ values for the first ring redox potentials of mixed substituted porphyrins is possibly due to the effect of the core metal ion and the nature of the mixed substituted porphyrin macrocycle. As reported earlier, the oxidation potentials are largely influenced by the substituent effect and nonplanarity of the porphyrin macrocycle while the reduction potentials are independent of structural change.[17,48,88] The planar structure[57a] of $H_2(TPP(Ph)_4)$ is anticipated to show variable degrees of nonplanarity with an increase in size or shape of the substituent X in $M(TPPR_4X_4)$ derivatives. The crystal structures of $Cu(TPP(Ph)_4(CH_3)_4)\cdot 2CHCl_3$ and $Zn(TPP(Ph)_4Br_4(CH_3OH))\cdot CH_3OH$ complexes showed considerable nonplanar conformation of the porphyrin ring. The ease of oxidation in mixed substituted porphyrins relative to the corresponding $M(TPPX_4)$ complexes has been ascribed to the electronic effects of the substituents and nonplanar distortion of the macrocycle; however, the reduction potentials are predominantly dependent on the nature of the substituents.

Table 7. Comparison of B Band and Q Band Transitions and HOMO−LUMO Gap ($\Delta E_{1/2}$) of Various Free-Base Porphyrins in CH_2Cl_2 at 298 K

porphyrin	B (nm)	$Q_x(0,0)$ (nm)	$Q_x(0,0)$ (eV)	$\Delta E_{1/2}$[b] (V)	ref
$(TPP(Ph)_4(CH_3)_4)$	457	704	1.76	1.79	*a*
$(TPP(Ph)_4Cl_4)$	463	717	1.73	1.77	*a*
$(TPP(Ph)_4Br_4)$	470	734	1.69	1.70	*a*
$(TPP(Ph)_4(CN)_4)$	464	778	1.59	1.41	*a*
$(TPP(Ph)_4)$	434	677	1.83	2.02	*a*
$(TPP(CH_3)_4Br_4)$	461	722	1.72	1.76	*a*
$(TPP(CH_3)_4(CN)_4)$	457	764	1.62	1.47	*a*
$(TPP(CH_3)_4)$	420	641	1.93	2.06	42, *a*
$(TPP(CH_3)_8)$	447	691	1.79	*c*	19
$(TPP(Ph)_8)$	468	724	1.71	*c*	89
$(TPPCl_8)$	452	720	1.72	*c*	90
$(TPPBr_8)$	469	743	1.67	1.64	25
(TPP)	414	646	1.92	2.23	7

[a] This work. [b] $\Delta E_{1/2}$ = [1]oxidation − [1]reduction. [c] Data not available.

A comparison of optical absorption spectral data and electrochemical redox potentials of the mixed substituted free-base porphyrins was made with the literature data of the porphyrins with similar β-pyrrole substituents, $H_2(TPP(X_8))$ compounds (X = Br, Cl, Ph, CH_3), and showed an interesting trend in their properties (Table 7). The $Q_x(0,0)$ transitions and $\Delta E_{1/2}$ of $H_2(TPPR_4X_4)$ compounds are intermediate in energy when compared to the parent analogues of similar β-pyrrole substituted-H_2TPP compounds. Qualitatively, the $\Delta E_{1/2}$ from the redox potentials correlates fairly well with the HOMO−LUMO gap calculated from the longest wavelength band in the electronic spectra of these derivatives.

Conclusions

In this article, two new families of mixed β-pyrrole substituted tetraphenylporphyrins have been reported. The mixed substituted free-base porphyrins and their metal complexes exhibited dramatic shift of the longest wavelength band relative to their corresponding $H_2(TPPR_4)$ (R = CH_3, Ph) or $H_2(TPPX_4)$ (X = H, Br, CN) derivatives. This has been attributed to the nature of the substituents and/or nonplanarity of the porphyrin ring. Crystal structures of $Cu(TPP(Ph)_4(CH_3)_4)$ and $Zn(TPP(Ph)_4Br_4)$ complexes showed nonplanar structure of the porphyrin ring and have been interpreted in terms of increased steric crowding; however, the nearly planar geometry of the porphyrin ring of a six-coordinated $Ni(TPP(Ph)_4(CN)_4(Py)_2)\cdot 2(Py)$ complex is probably due to the decreased steric repulsive interactions among the peripheral substituents. Electrochemical redox potentials of these porphyrins showed dramatic variation and span a wide range in first ring oxidation (0.38−1.36 V) and in reduction (−0.28 to −1.5 V) potentials. The redox potentials were analyzed by Hammett plots, and it was found that the

(86) Ghosh, A.; Halvorsen, I.; Nilsen, H. J.; Steene, E.; Wondimagegn, T.; Lie, R.; Van Caemelbecke, E.; Guo, N.; Ou, Z.; Kadish, K. M. *J. Phys. Chem. B* **2001**, *105*, 8120.
(87) (a) Walker, F. A.; Beroiz, D.; Kadish, K. M. *J. Am. Chem. Soc.* **1976**, *98*, 3484. (b) Kadish, K. M.; Morrison, M. M. *J. Am. Chem. Soc.* **1976**, *98*, 3326.
(88) Takeuchi, T.; Gray, H. B.; Goddard, W. A., III. *J. Am. Chem. Soc.* **1994**, *116*, 9730.
(89) Medforth, C. J.; Senge, M. O.; Smith, K. M.; Sparks, L. D.; Shelnutt, J. A. *J. Am. Chem. Soc.* **1992**, *114*, 9859.
(90) Wijesekara, T.; Dupre, D.; Cader, M. S. R.; Dolphin, D. *Bull. Soc. Chim. Fr.* **1996**, *133*, 765.

extent of HOMO−LUMO gap decreases with increase in the Hammett parameter of the substituents. The similarity in reduction rather than in oxidation potentials of mixed substituted porphyrins $M(TPPR_4X_4)$ ($R = Ph, CH_3$; $X = Br, CN$) relative to the corresponding $M(TPPX_4)$ has been interpreted in terms of the greater effect of substituent X on the LUMO levels and nonplanarity of the porphyrin macrocycle and/or substituent effects on the HOMO levels of the porphyrin π-system.

Acknowledgment. This work was supported by the funds from the Council of Scientific and Industrial Research (CSIR) and in part by the Defense Research Development Organisation (DRDO), Government of India (to P.B.).

Supporting Information Available: Tables of optical absorption and electrochemical redox data of $MTPP(CH_3)_4X_4$ derivatives; bond lengths, bond angles, and anisotropic thermal parameters for $Cu(TPP(Ph)_4(CH_3)_4)\cdot 2(CHCl_3)$, $Zn(TPP(Ph)_4Br_4(CH_3OH))\cdot(CH_3OH)$, and $Ni(TPP(Ph)_4(CN)4(Py)_2)\cdot 2(Py)$ complexes and their crystallographic information file in CIF format. This material is available free of charge via the Internet at http://pubs.acs.org.

IC052035B